Chapter 4
Scanning Tunneling Spectroscopy

Objective: to learn the implementation principles of STM spectroscopy and some of its main applications

The spectroscopy mode

Measuring the differential conductance gives access to the LDOS.

$$\frac{dI}{dV} \propto \int_{-\infty}^{+\infty} N_B(E) \frac{df(E-eV)}{dV} dE$$

If T = 0: $\frac{dI}{dV}(V) \propto N_B(E_F - eV)$

A perfect stability is required:

If the tip-sample distance varies by Δz, then the current I varies by ΔI:

$$\frac{\Delta I}{I} = 2\alpha\Delta z = 2\frac{\sqrt{2mW}}{\hbar}\Delta z$$

with $\alpha \approx 1 Å^{-1}$

To avoid this mechanical noise down to below 1% of relative variation $\Delta I/I$ requires Δz below 0.5 pm, i.e. a pm-scale mechanical stability.

The spectroscopy mode

How to make a spectroscopy experiment ? First:

- Position the tip
- Freeze height regulation

Second:

- Measure I(V)
- Differentiate to get dI/dV, which measures the sample LDOS

OR

- Add a bias modulation dV. $V = V_{dc} + V_{ac0} \cos \omega t$
- Measure ac current response amplitude as a function of V_{dc}.

$$I = I(V_{dc}) + \left.\frac{dI}{dV}\right|_{V=V_{dc}} .V_{ac0} \cos \omega t$$

Chapter 4
Scanning Tunneling Spectroscopy

4.1 Superconductors

Elements of superconductivity (1)

A superconductor (below T_c, I_c and B_c):
zero resistance,
perfect diamagnetism (B = 0),
modified density of states at the FL,

BCS theory : the DOS writes :

$$N_S(E) = 0 \quad \text{if} \left|E - E_F\right| < \Delta$$

$$N_S(E) = N_N \frac{\left|E\right|}{\sqrt{(E - E_F)^2 - \Delta^2}} \quad \text{if} \left|E - E_F\right| > \Delta$$

The energy gap is :
$\Delta(T->0) = 1.76 k_B T_c$

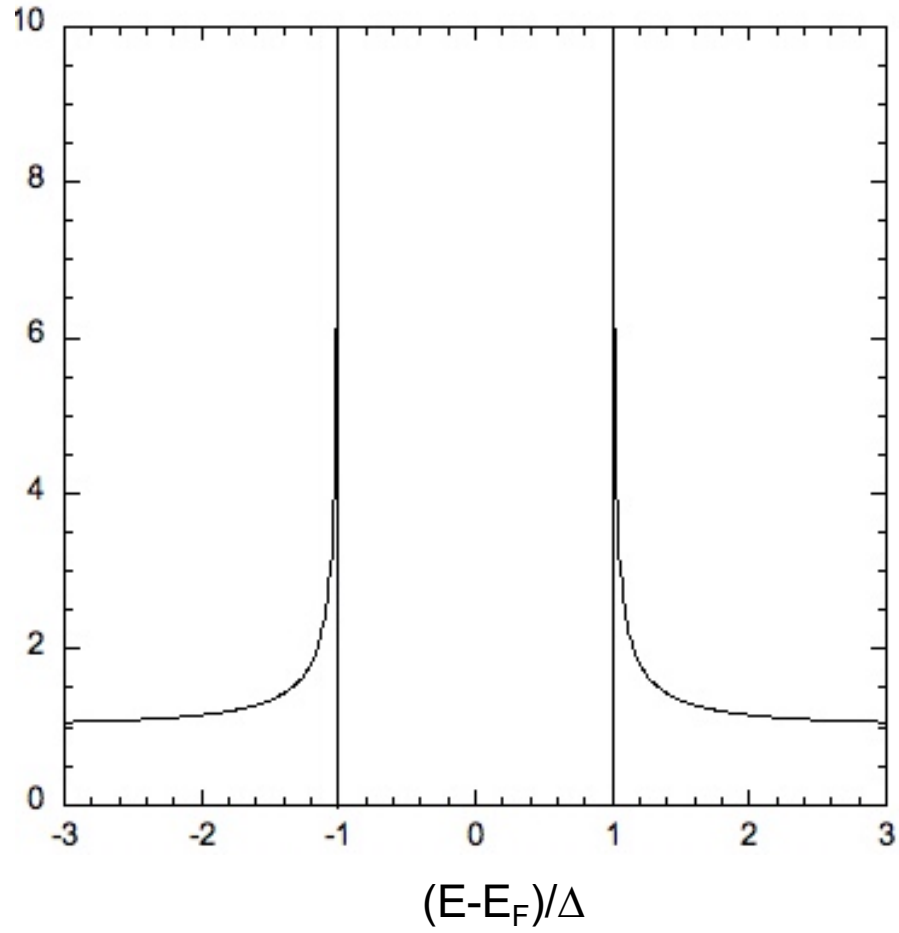

$NbSe_2$

Lamellar compound,

Easy to cleave (scotch tape): gives a clean, inert surface.

Superconducting below 7.2 K.

Spectra follows BCS shape.

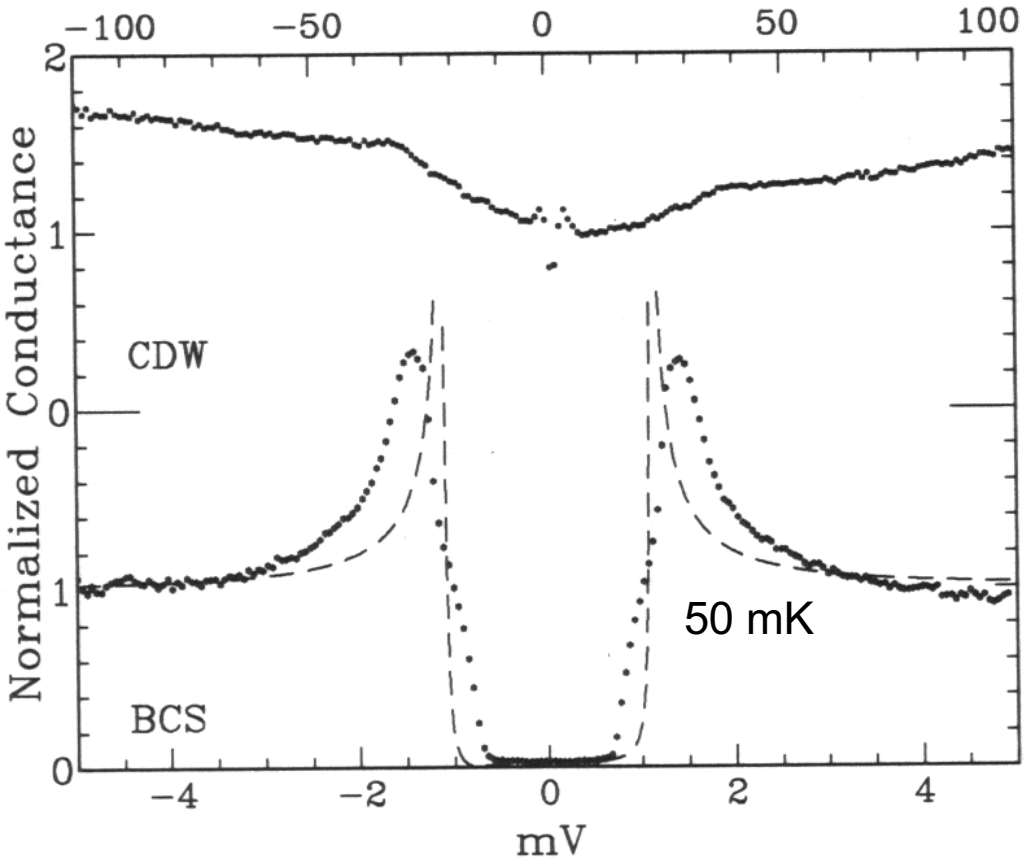

H.F. Hess et al., Physica B 169, 422 (1991).

Elements of superconductivity (2)

A superconductor under magnetic field: magnetic field penetrates as vortices made of a normal core,each vortex carries a flux quantum ϕ_0.

$$\phi_0 = \frac{h}{2e} = 2.0\,10^{-15}\,\mathrm{T.m^2} = 2.0\,\mathrm{mT.\mu m^2}$$

When field increases, the number of vortices increases accordingly.

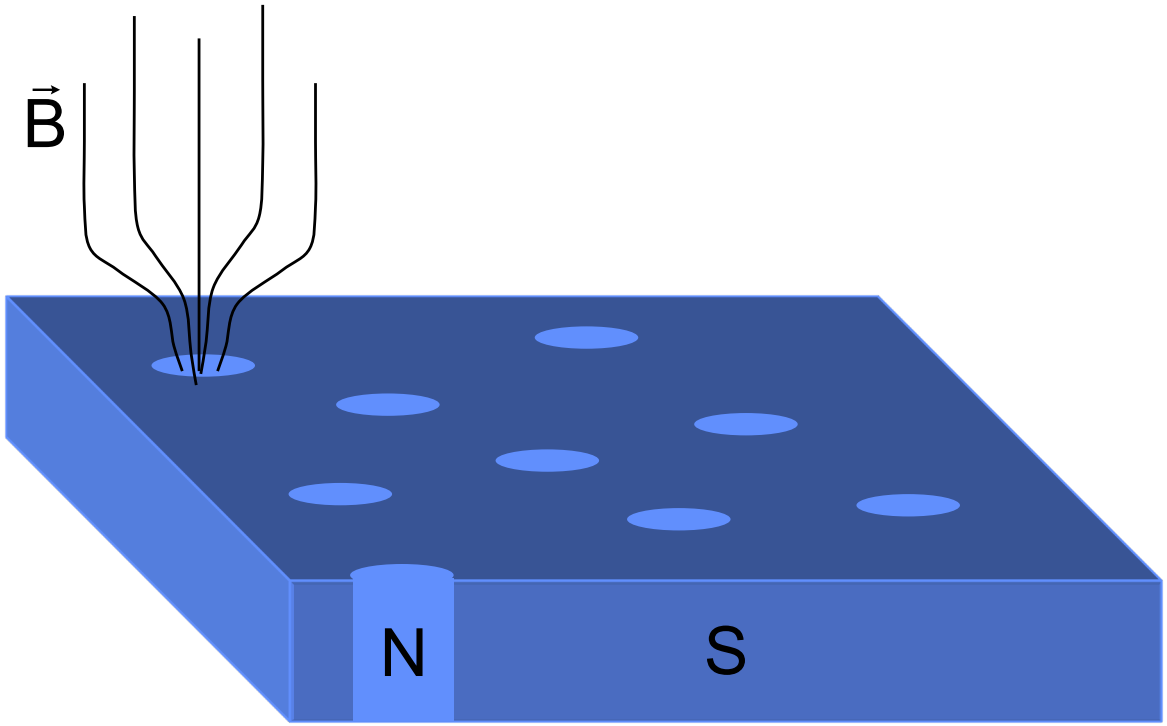

Inside a vortex

Local magnetic field depletes Cooper pair density and pairing potential.

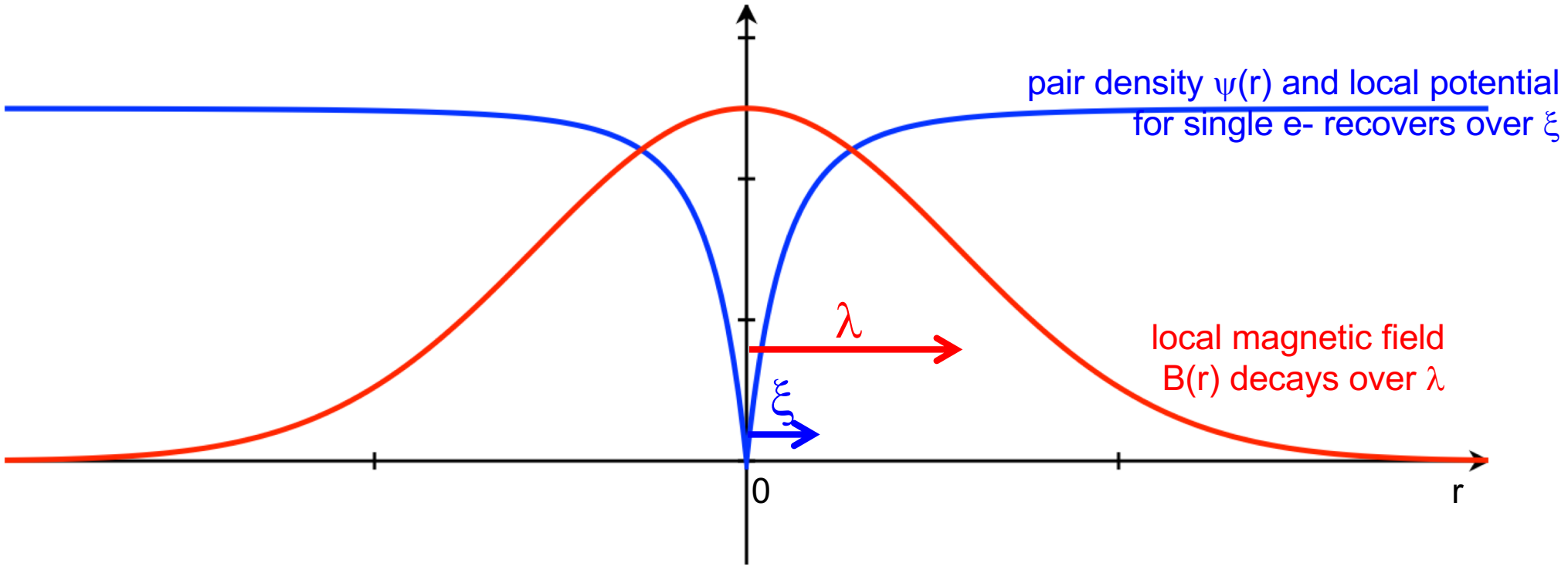

Magnetic field decays on the penetration length λ_L,

Pair density decays on the coherence length ξ_s.

In type II superconductor: $\lambda_L > \xi_s$: a vortex is energetically favored compared to full screening. In NbSe2, : ξs = 77 Å, λL = 2000 Å.

Inside a vortex

Local magnetic field depletes Cooper pair density and pairing potential.

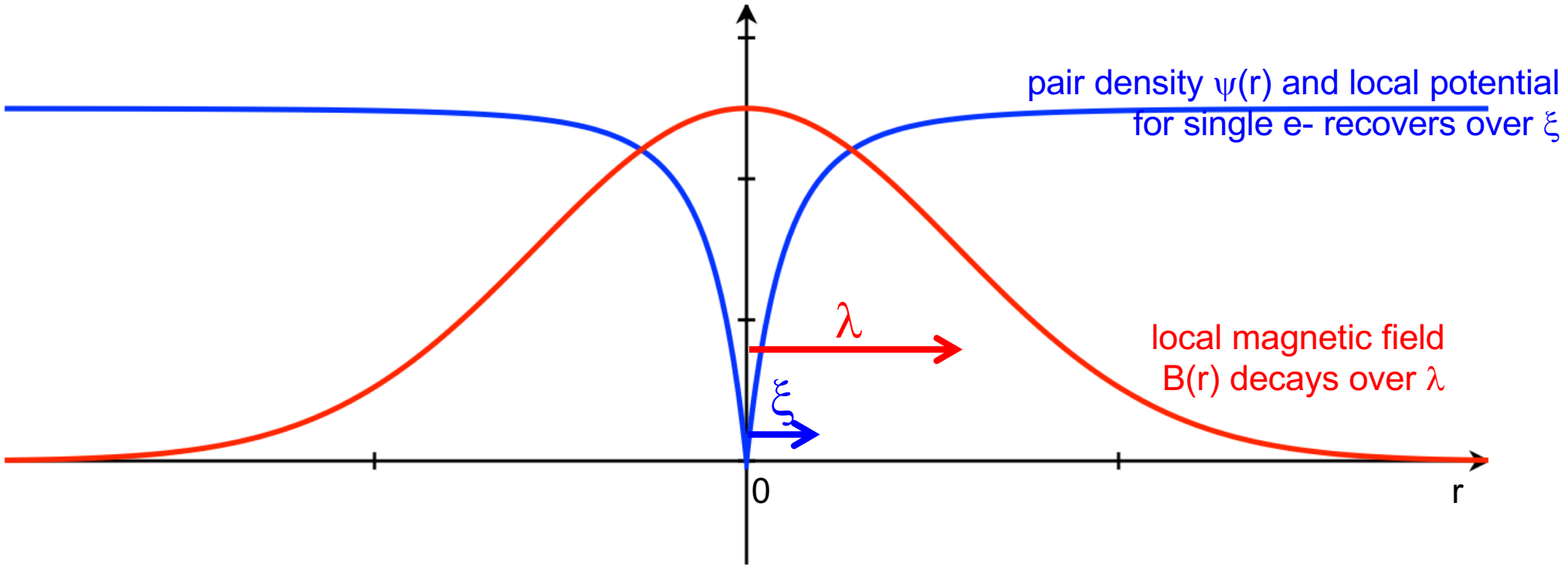

Screening currents around a single point: a vortex.

Localized (single-)electron states, local density of states modified.

Localized states in a vortex

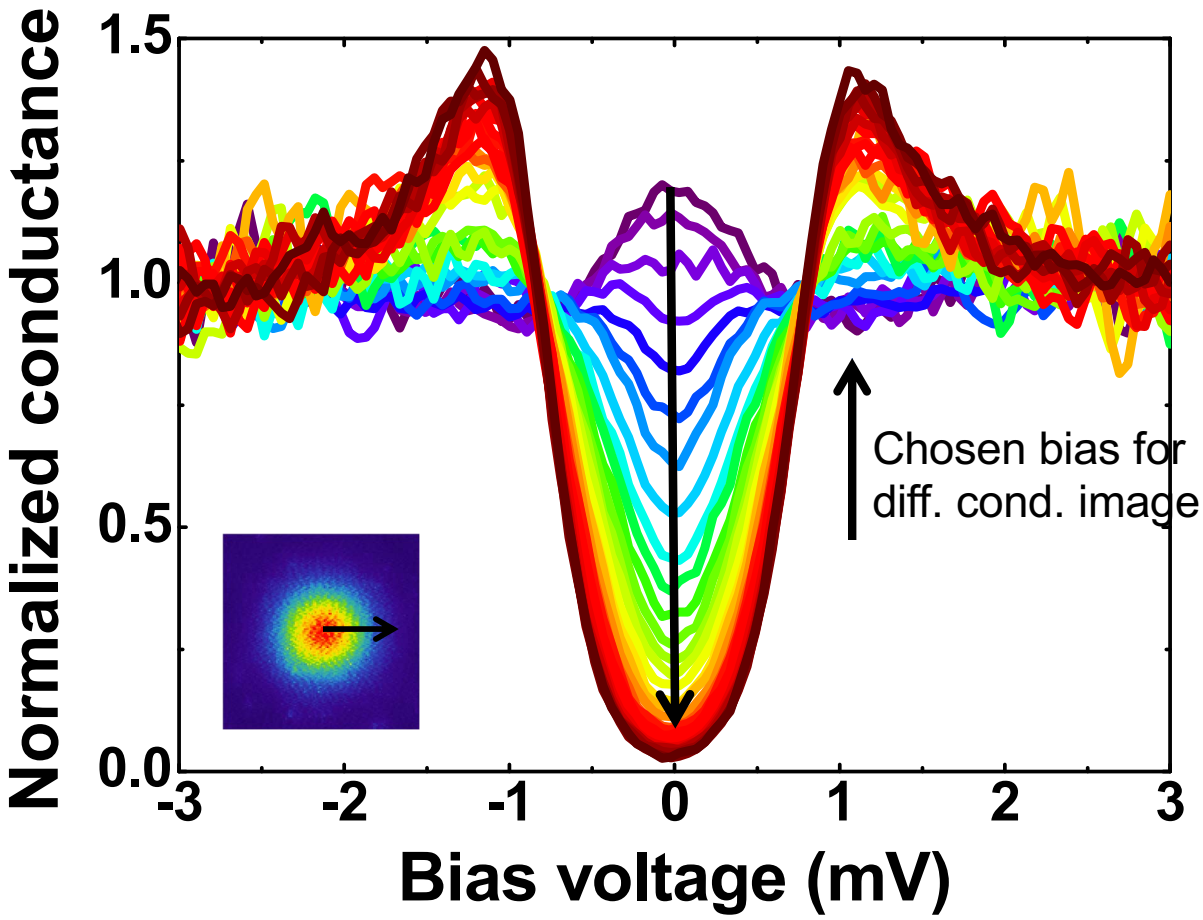

Series of LDOS spectroscopy along a line across a vortex: quasiparticules states confined within a vortex core = LDOS peak.

A. Fente, H. Suderow et al., Phys. Rev. B **94**, 014517 (2016).

The differential conductance imaging

During scan: ac modulation V_{ac} added to dc bias V_{dc}.

$$V = V_{dc} + V_{ac0} \cos \omega t$$

Regulation slower than ac modulation ⇒ ac current modulation.

$$I = I\left(V_{dc}\right) + I_{ac} \cos \omega t = I\left(V_{dc}\right) + \left.\frac{dI}{dV}\right|_{V=V_{dc}} .V_{ac0} \cos \omega t$$

(first order expansion of I(V)).

dI is measured and displayed (with grey levels).
Bias V_{dc} well chosen so that dI/dV image reflects the LDOS structure.

Also called STS map.

The vortex lattice

Abrikosov (Nobel 2003) vortex lattice.

Triangular geometry: interaction between vortices is minimized.

Vortex density determined by the magnetic field.

H.F. Hess et al., Phys. Rev. Lett. 62, 214 (1989).

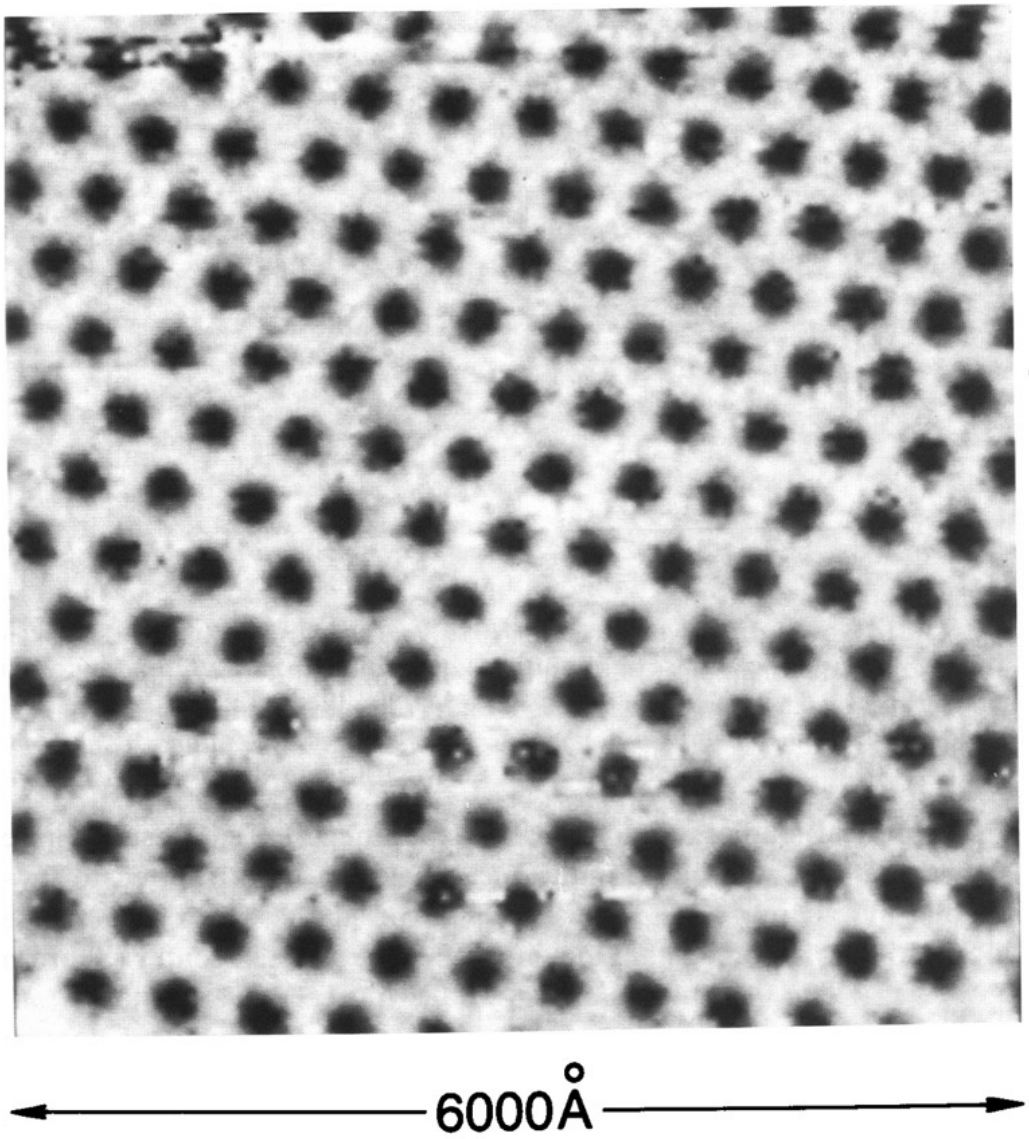

Fig. 4.120. Abrikosov flux lattice produced by 1 T magnetic field in $NbSe_2$ at 1.8 K. The gray scale corresponds to d*I*/d*U* (Hess *et al.*, 1989).

The vortex lattice

Abrikosov (Nobel 2003) vortex lattice.

Triangular geometry: interaction between vortices is minimized.

Vortex density determined by the magnetic field.

I. Guillamon, H. Suderow et al., Phys. Rev. Lett. 101, 166407 (2008).

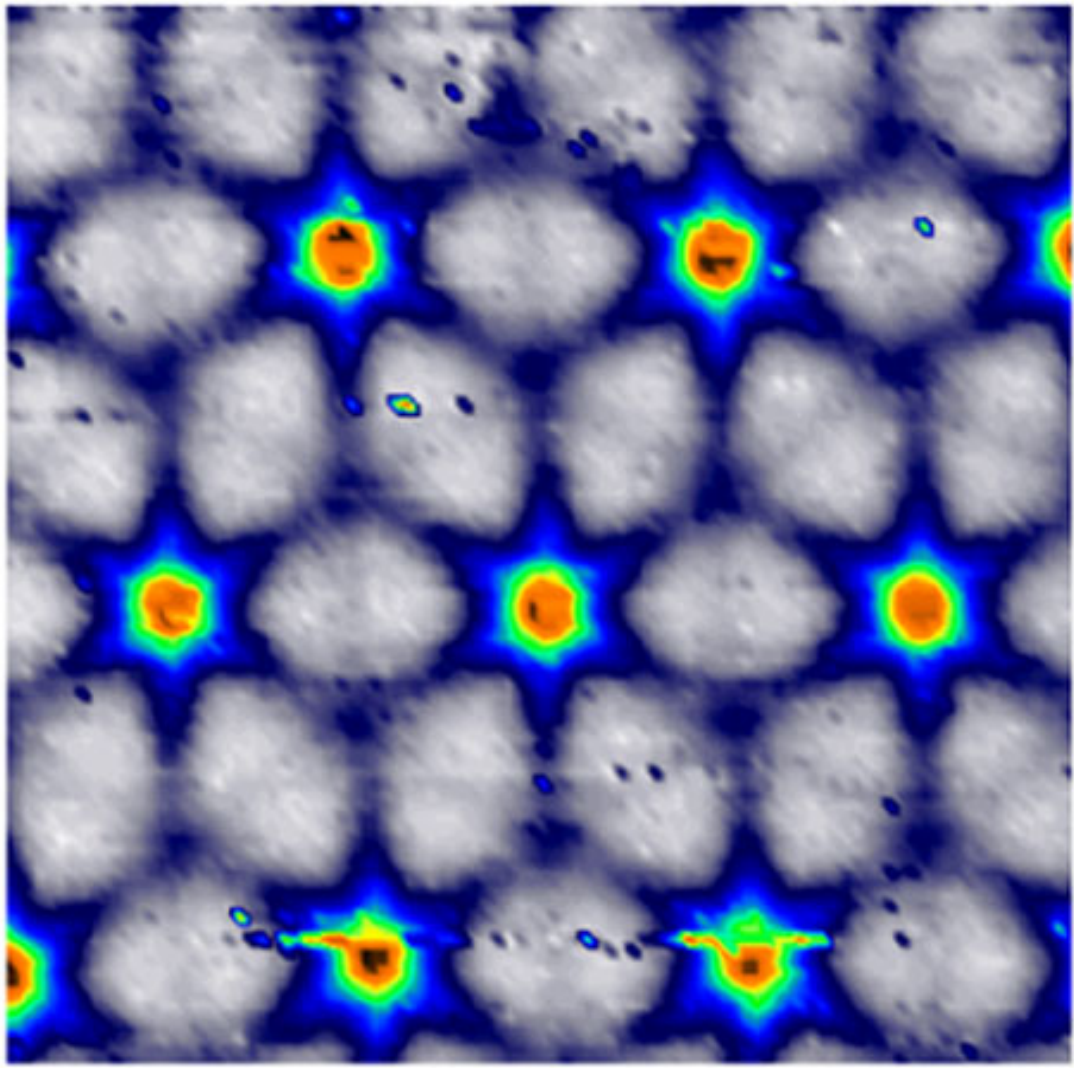

360 x 360 nm^2, 0.1 K, 0.15 T

High-Tc superconductors

Ceramics made of CuO_2 planes and rare earth elements.

d-wave condensate, strong disorder.

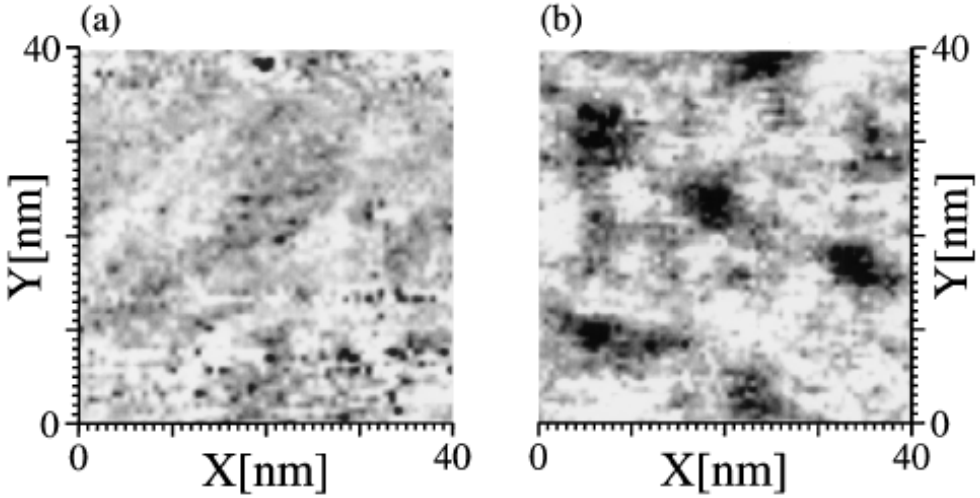

FIG. 1. STS maps of the conductance at $V = -\Delta_p/e$ at 4.2 K on overdoped BSCCO ($T_c = 74.3$ K); white and dark correspond to large and low conductance, respectively: (a) $B = 0$ T; (b) $B = 6$ T.

= diff. cond. map

I. Maggio-Aprile et al, Phys. Rev. Lett. 80, 3606 (1998).

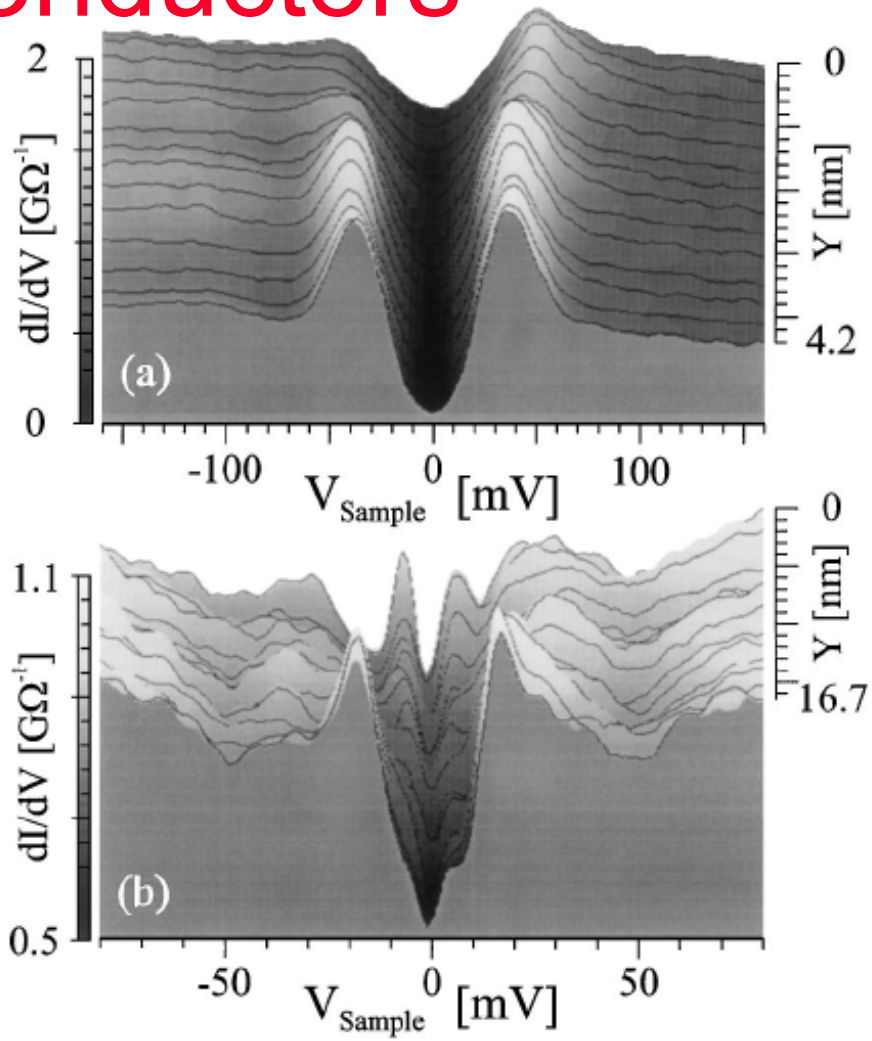

FIG. 2. Three dimensional view of tunneling spectra measured at equally spaced positions along a line extending from the center of a core ($Y = 0$) to a point located away from the vortices at 4.2 K and 6 T. (a) 4.2 nm trace on overdoped BSCCO ($T_c = 74.3$ K). (b) 16.7 nm trace on optimally doped YBCO ($T_c = 91$ K). Note the difference by a factor of 2 in the energy scales and the large zero bias conductance in YBCO.

Superconducting polycrystalline Boron-doped Diamond (poly-BDD)

Prepared by Microwave Plasma Enhanced Chemical Vapor Deposition: MWPECVD.

Sample	Substrate	Thickness	Resistivity	T_C
A	Quartz	1 μm	26 m$\Omega\cdot$ cm	2 K
B	SiO_2/Si	200 nm	12 m$\Omega\cdot$ cm	3 K

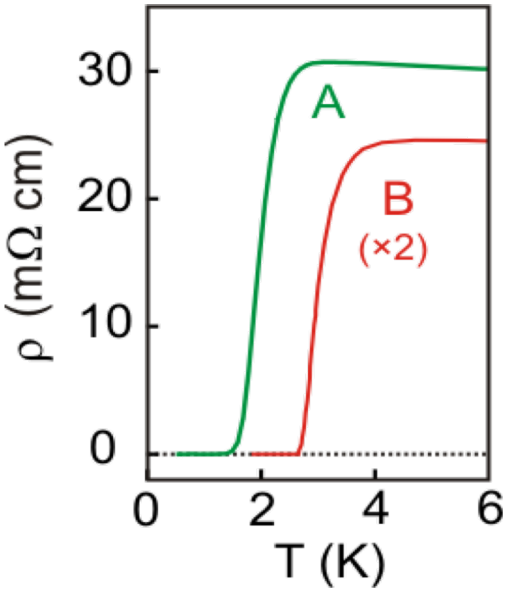

TEM cross-section image

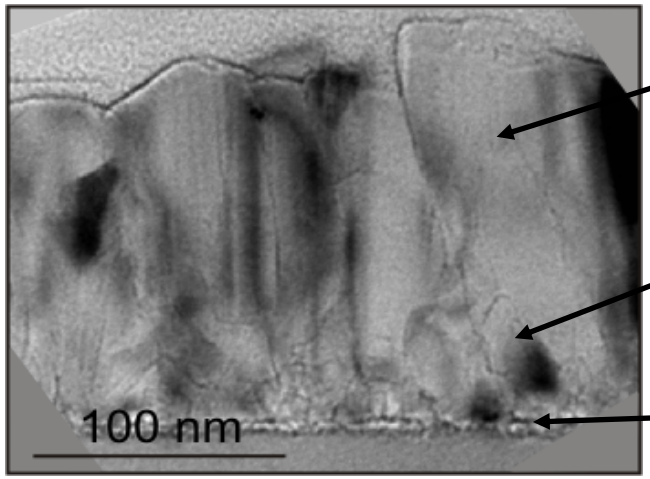

Large columnar grains in (111) and (001) crystallographic orientations,

Randomly oriented small grains nucleated on the seeds,

Diamonds seeds (nm size).

O. A. Williams et al., Diamond & Related Materials 17, 1080 (2008).

Poly-BDD tunneling spectroscopy

Topography

Granular morphology:
average height 80 nm,
size less than 150 nm

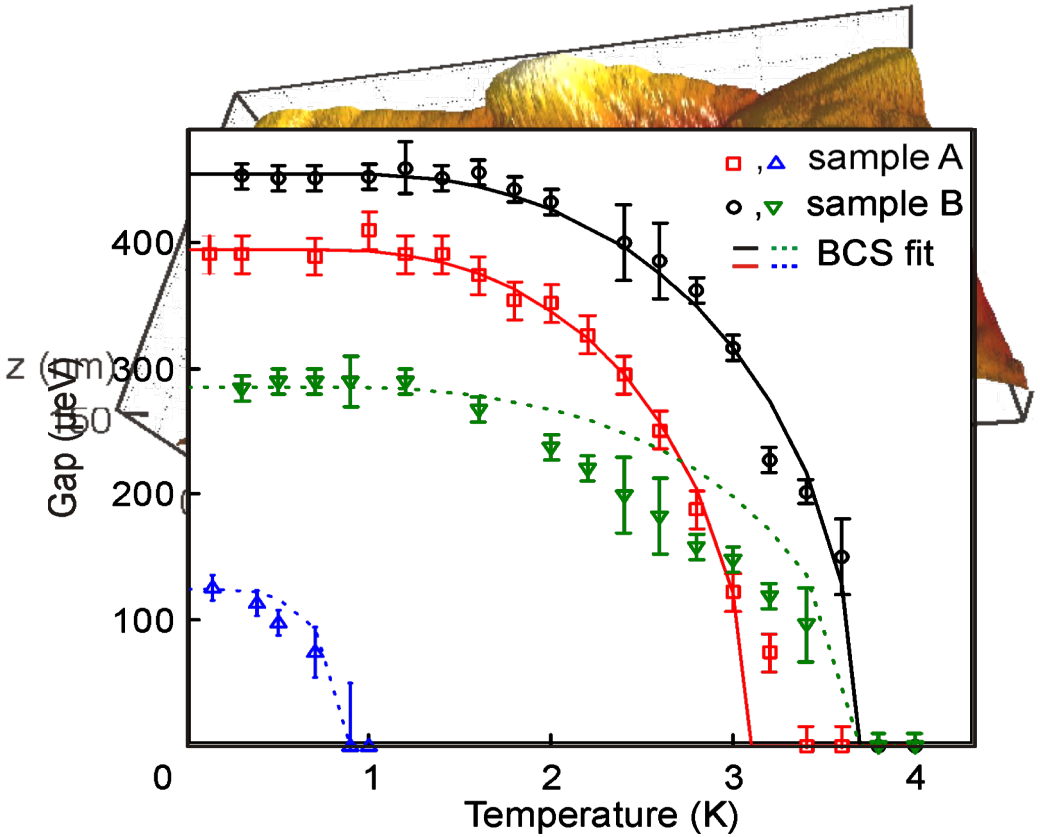

Spectroscopy

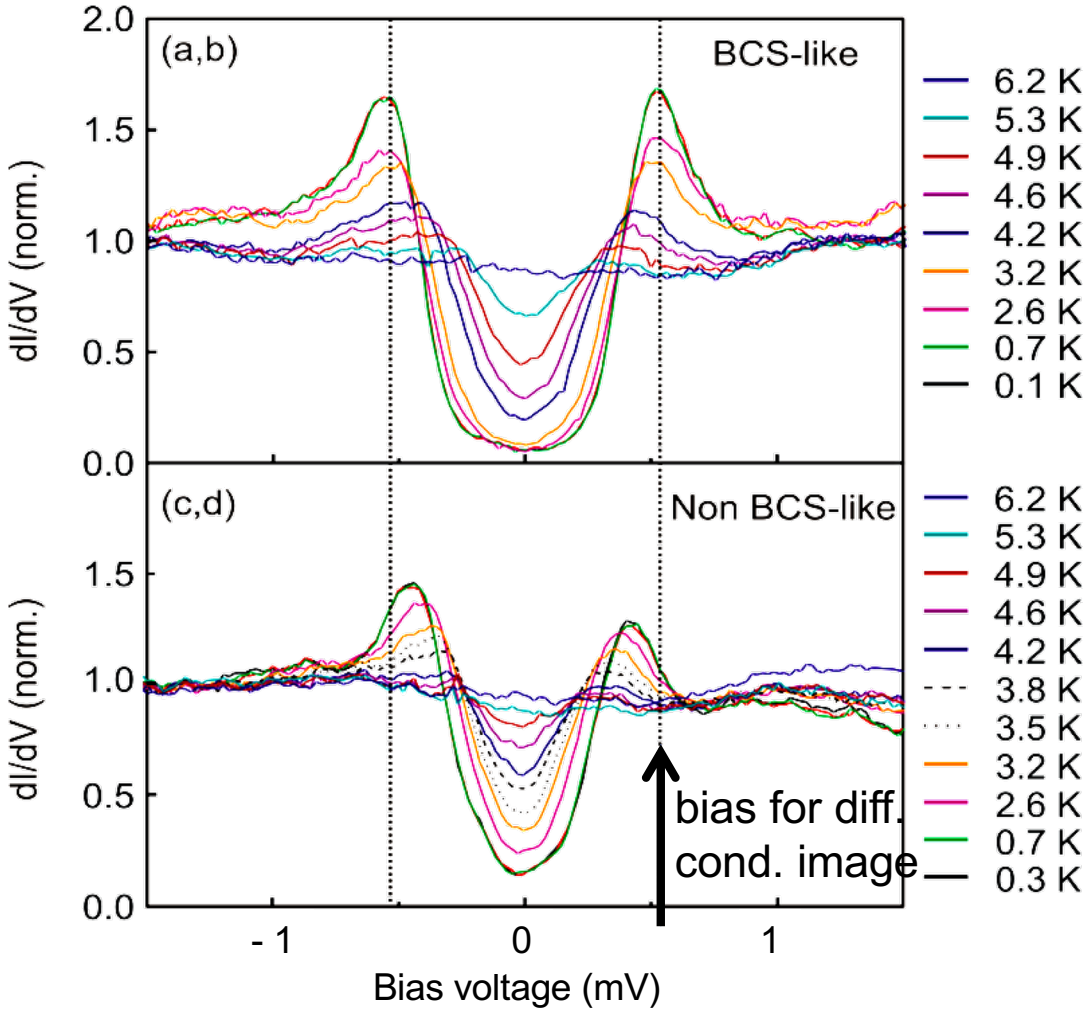

Different electrical properties: BCS (a,b) and non-BCS superconductivity (c,d)

Microstructure superconductivity correlation

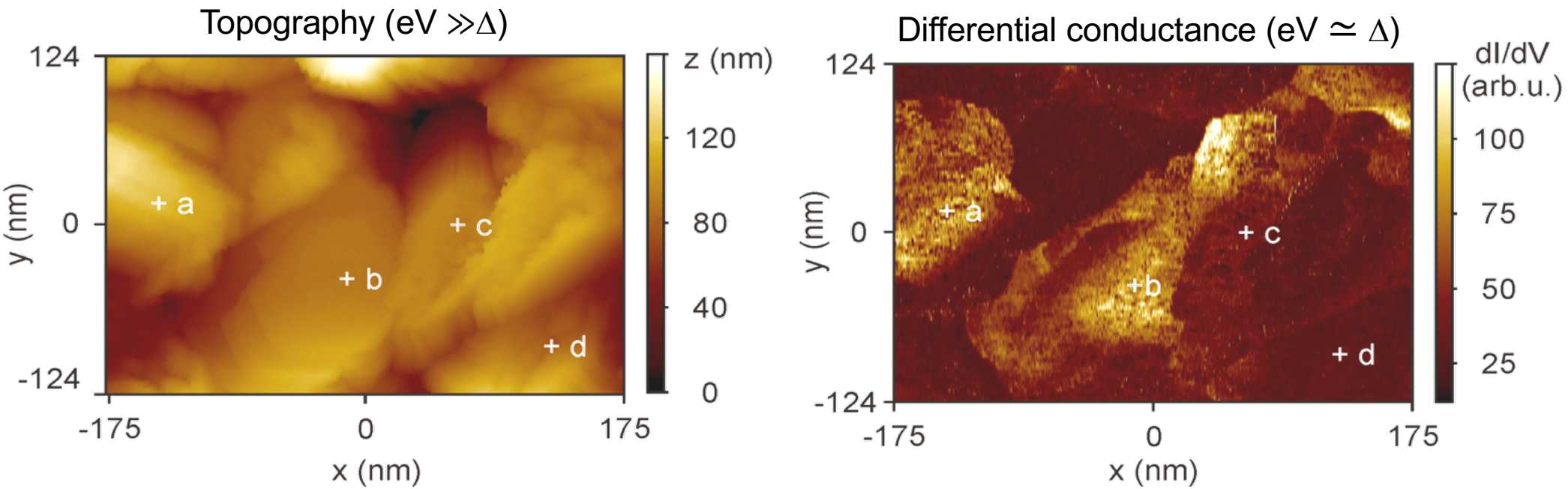

Superconducting properties follow the film morphology !

Poly-BDD = disordered network of BCS and non-BCS superconducting grains, proximity effect relevant.

Model system for strongly disordered superconductors.

Applications for innovative superconducting devices.

F. Dahlem, H. Courtois et al., Phys. Rev. B 82, 033306 (2010).

Chapter 4
Scanning Tunneling Spectroscopy

4.2 Inelastic Electron Tunneling Spectroscopy (IETS)

Inelastic tunneling spectroscopy (1)

Tunneling is usually elastic.

An inelastic channel can appear in some cases.

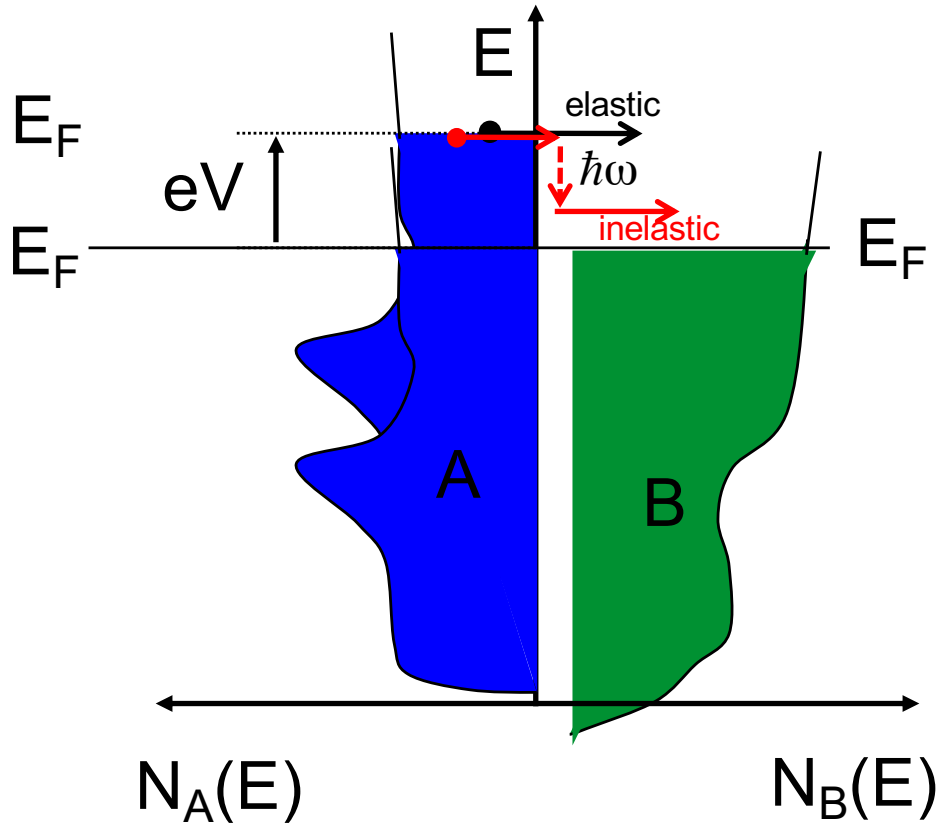

An energy $\hbar\omega$ is emitted as a phonon or a photon.

Threshold defined by the excitation energy.

$$|eV| > \hbar\omega$$

Inelastic tunneling spectroscopy (1)

Tunneling is usually elastic.

An inelastic channel can appear in some cases.

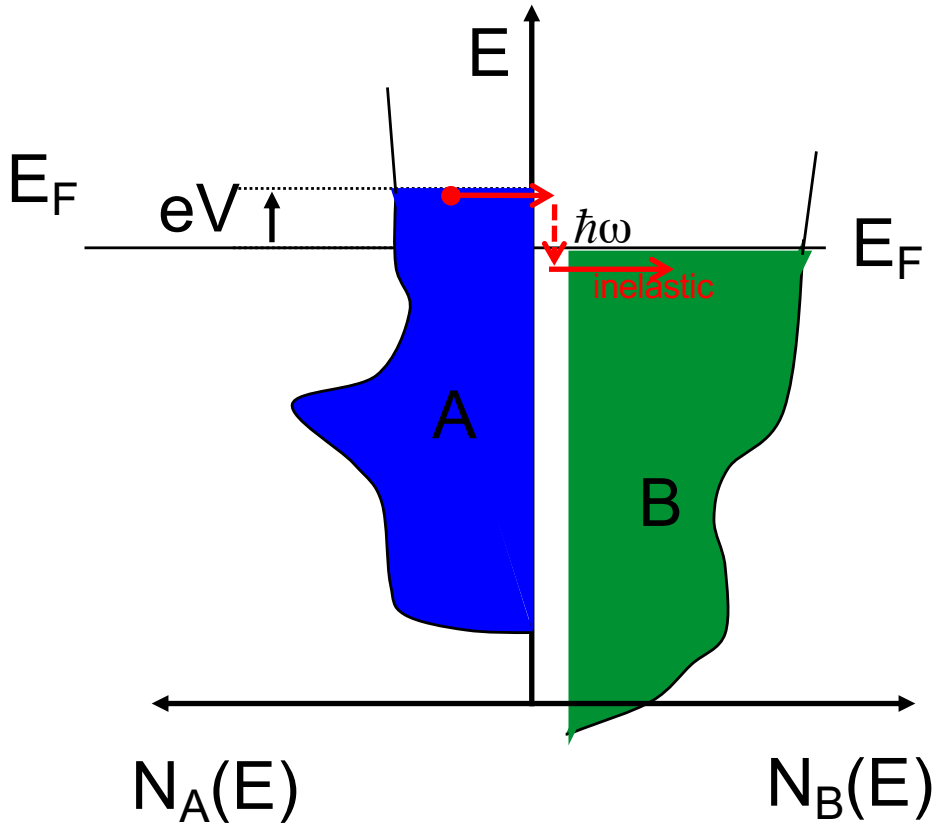

An energy $\hbar\omega$ is emitted as a phonon or a photon.

Threshold defined by the excitation energy.

$$|eV| > \hbar\omega$$

Inelastic tunneling spectroscopy (2)

Change in current too small to be measured in I-V. More easily accessed in second derivative.

W. Ho, J. Chem. Phys. 117, 11033 (2002)

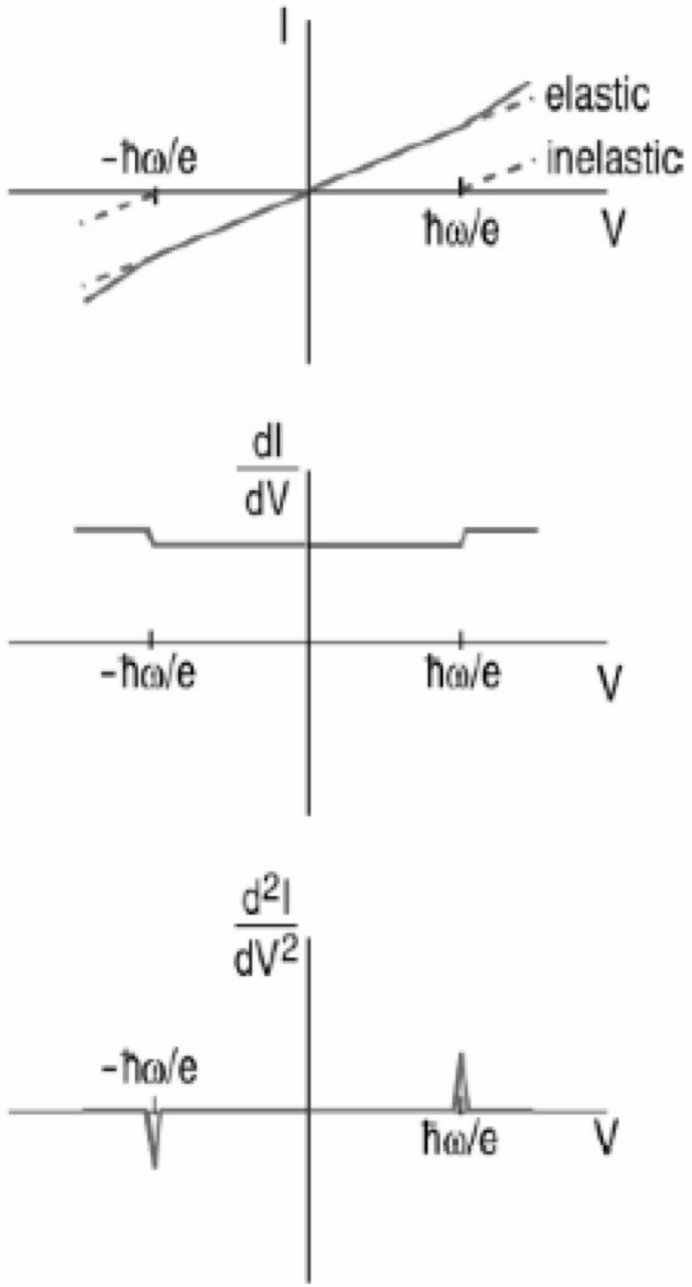

Inelastic tunneling spectroscopy (3)

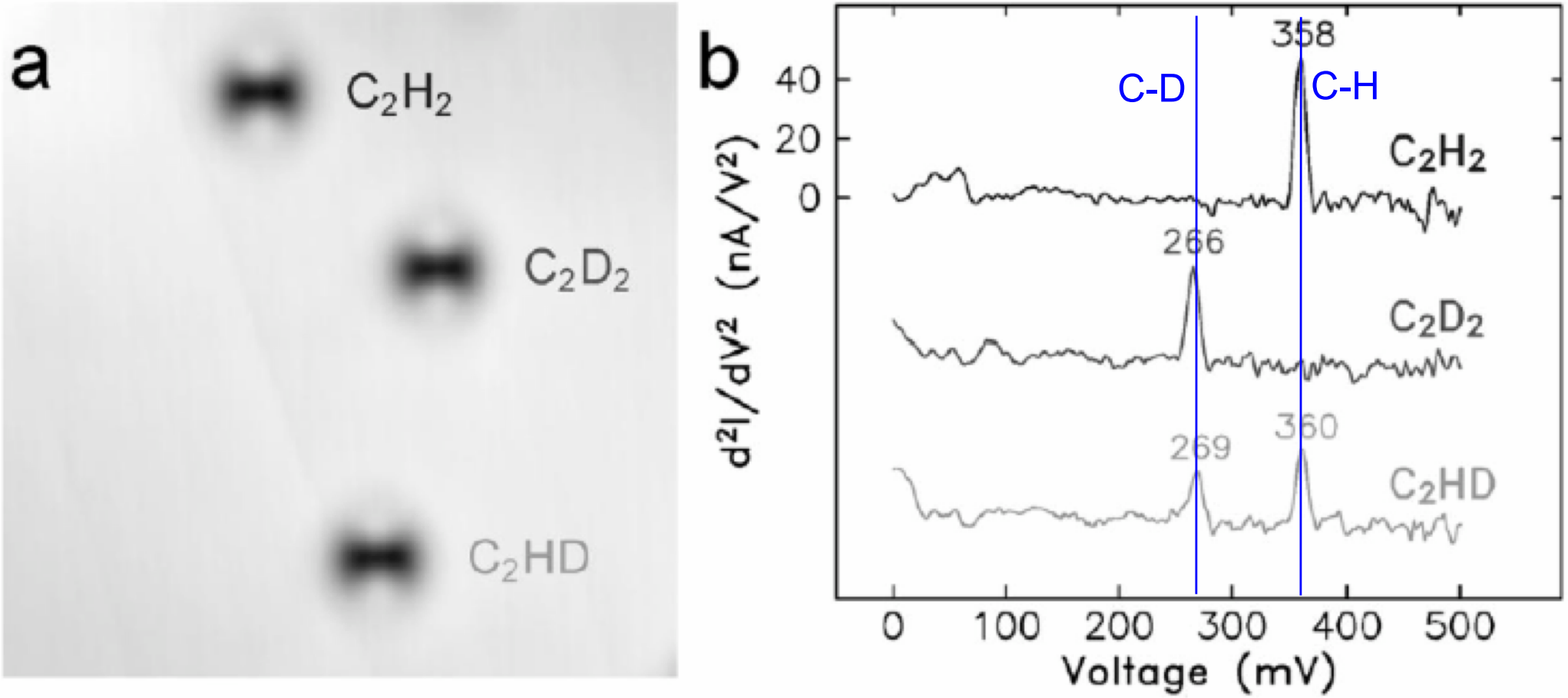

Isotopes can be distinguished: single bond sensitivity of STM-IETS.

B.C. Stipe, M.A. Rezaei, and W. Ho, Science 280, 1732 (1998).
56 x 56 Å^2 STM image and STM-IETS spectra of acetylene isotopes on Cu(001), 8 K.
Bright protrusions are the C–H,D bonds, the central depression dark is the C–C bond.

Chapter 4
Scanning Tunneling Spectroscopy

4.3 Graphene

Electronic states in graphene (1)

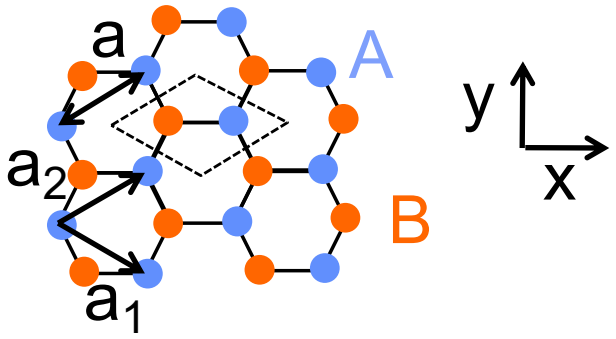

Two atoms per unit cell (diamond),
A and B.
a = 0.246 nm

sp^2: s, p_x and p_y hybridize to form σ states, which are in-plane, occupied by 3 electrons. p_z states allow conduction: to be considered in the following, occupied by one electron per atom.

Tight binding approx.: electrons tighly bound to their atom, electronic states are a combination of p_z atomic orbital.

Electronic states in graphene (2)

Let's build Bloch states: $$\left|\psi_s^k\left(\vec{r}\right)\right\rangle = \frac{1}{\sqrt{N}}\sum_{i\in s} e^{i\vec{k}.\vec{r}(i)}\left(c_i^s\right)^+\left|0\right\rangle$$

Hamiltonian includes hopping between every A (B) site and its neighbors.

$$H = -t\sum_{i\in A}\sum_{a=1,2,3}\left[\left(c_{i+a}^B\right)^+ c_i^A + \left(c_i^A\right)^+ c_{i+a}^B\right]$$

sub-lattice A → $i\in A$

$a=1,2,3$ ← 3 neighbours per atom

We calculate:

$$\left\langle\psi_A^k\left|H\right|\psi_B^k\right\rangle = -t\sum_{a=1,2,3} e^{i\vec{k}.\vec{r}_a} = t.f\left(\vec{k}\right) \quad \text{and} \quad \left\langle\psi_B^k\left|H\right|\psi_A^k\right\rangle = t.f^*\left(\vec{k}\right)$$

Lattice geometry gives:

$$\vec{r}_1\begin{vmatrix}0\\ a/\sqrt{3}\end{vmatrix} \qquad \vec{r}_2\begin{vmatrix}-a/2\\ -a/2\sqrt{3}\end{vmatrix} \qquad \vec{r}_3\begin{vmatrix}a/2\\ -a/2\sqrt{3}\end{vmatrix}$$

We have:

$$\left\langle\psi_A^k\left|H\right|\psi_A^k\right\rangle = \left\langle\psi_B^k\left|H\right|\psi_B^k\right\rangle = 0$$

Electronic states in graphene (2)

Shrödinger equation writes:

$$-t\begin{pmatrix} 0 & f(\vec{k}) \\ f(\vec{k})^{*} & 0 \end{pmatrix}\begin{pmatrix} |\psi_A^k\rangle \\ |\psi_B^k\rangle \end{pmatrix} = E(\vec{k})\begin{pmatrix} |\psi_A^k\rangle \\ |\psi_B^k\rangle \end{pmatrix}$$

Hamiltonian diagonalization gives: $E(\vec{k}) = \pm t\left|f(\vec{k})\right|$

One finds:

$$\left|f(k)\right| = \left[3 + 2\cos(k_y a) + 4\cos\left(\sqrt{3}k_x a/2\right)\cos(k_y a/2)\right]^{1/2}$$

$$E(k) = \pm t\left[3 + 2\cos(k_y a) + 4\cos\left(\sqrt{3}k_x a/2\right)\cos(k_y a/2)\right]^{1/2}$$

Electronic states in graphene (3)

$$E(k) = \pm t\left[3 + 2\cos(k_y a) + 4\cos\left(\sqrt{3}k_x a/2\right)\cos(k_y a/2)\right]^{1/2}$$

t = 2.5 eV (nearest neighbour transfer integral), zero defined at the Fermi level.

1 e- / atom in binding orbital E < 0.

Fermi level made of 6 points K: intrinsic graphene is a semi-metal or gapless semiconductor.

Close to FL, linear relation dispersion: Dirac fermions.

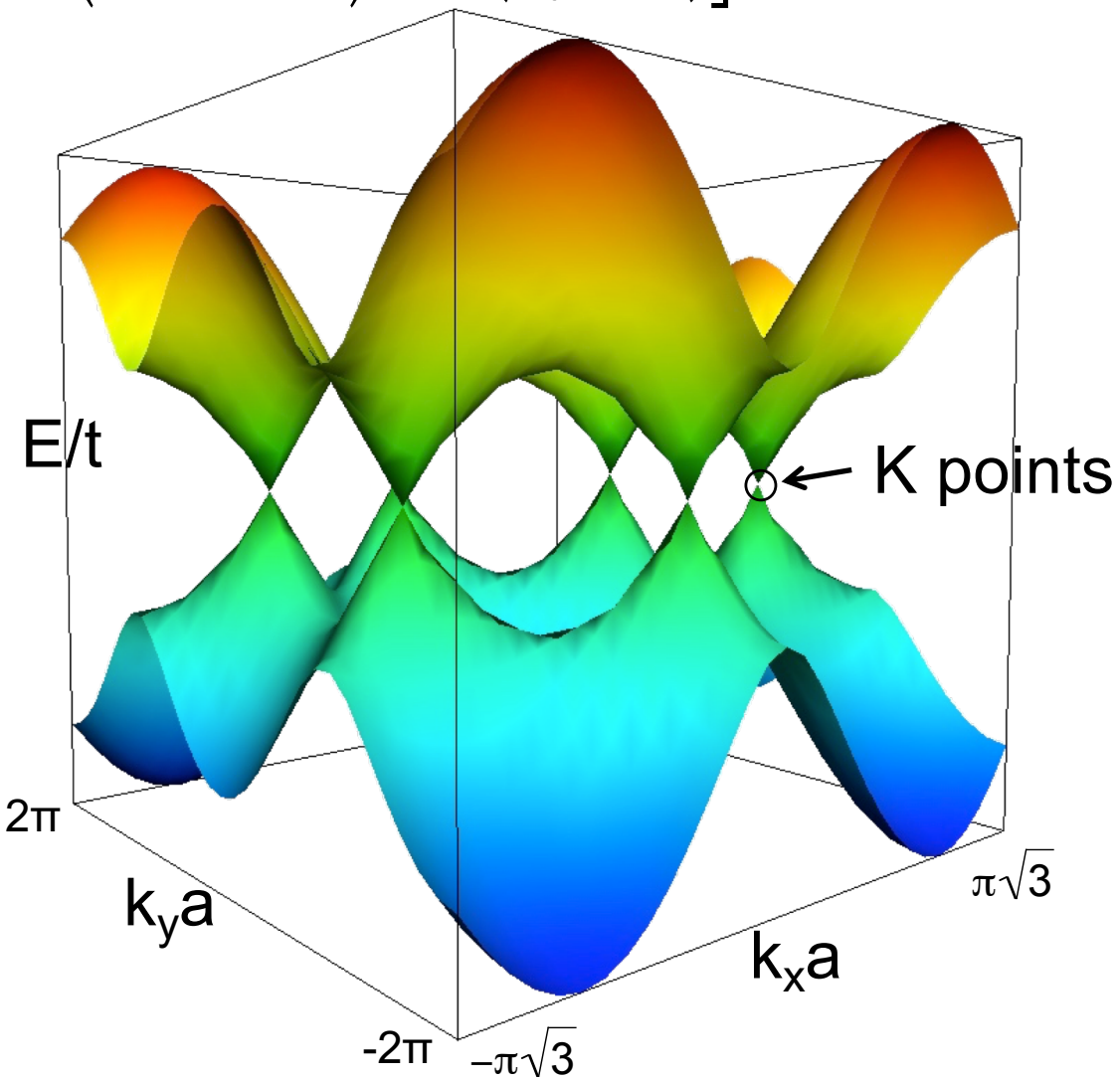

P. R. Wallace, Phys. Rev. 71, 622 (1947).

Topographic disorder and density of states in graphene on Ir (111) after exposure to air

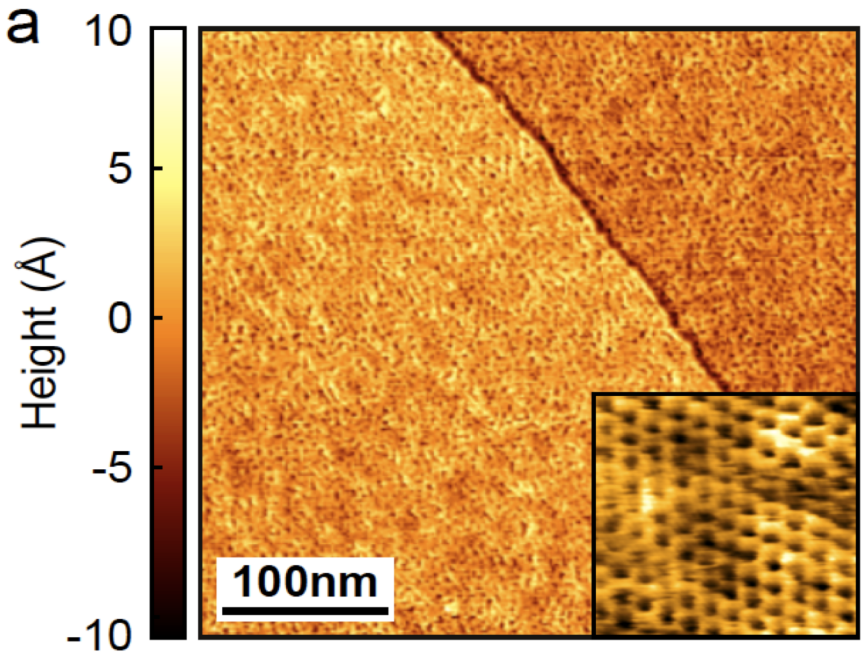

Atomic resolution: clean surface
No moiré
Surface roughness $\sigma_z \approx 100$ pm

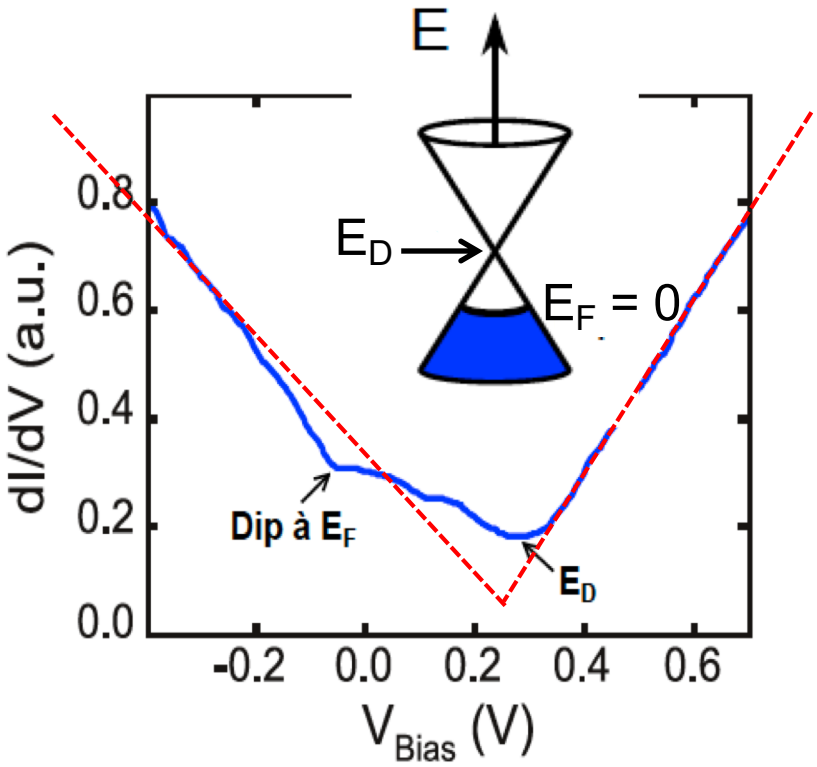

Local density of states is V-shaped
Minimum at $eV=E_D$ indicates the **local doping level,** here p type

Position dependence of the doping

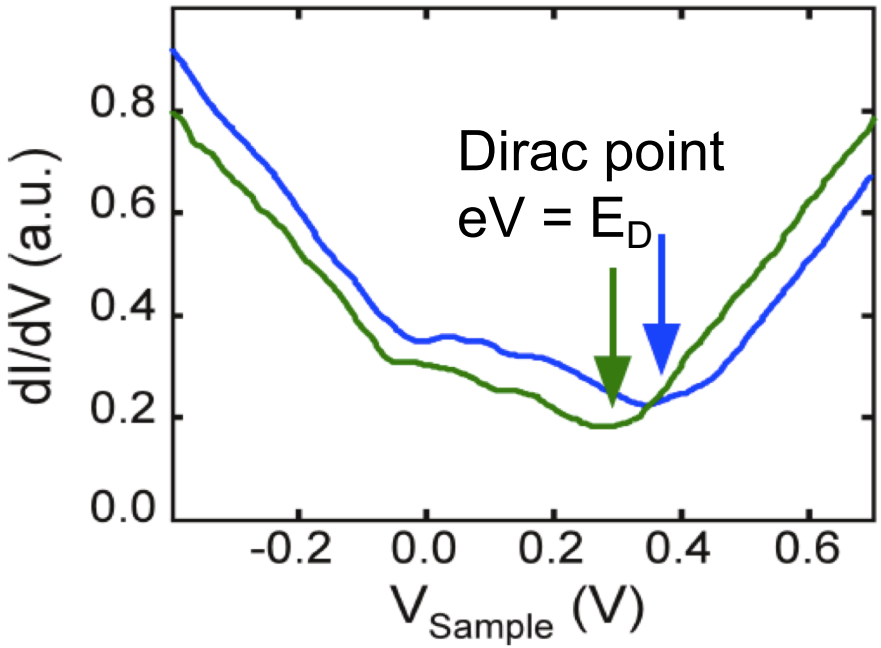

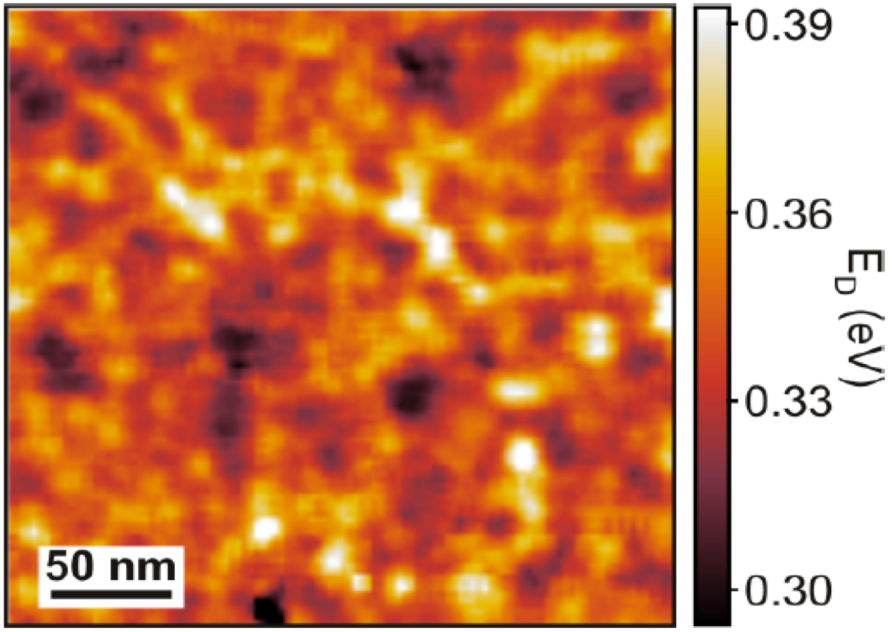

11 000 spectra, ~32h

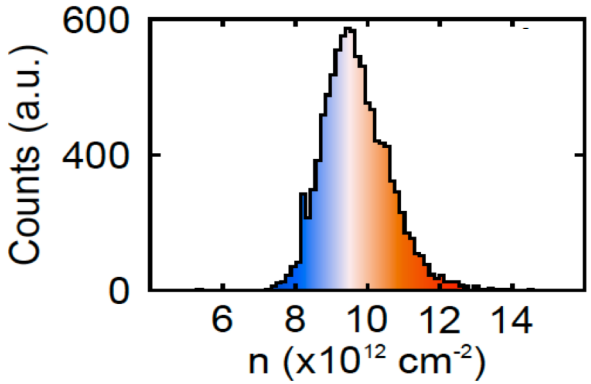

LDOS maps: extract $E_D(\mathbf{r})$, convert in local doping:

$$E_D = \hbar v_F \sqrt{\pi n}$$

$E_D^0 = 340$ meV, $n \approx 10^{13}$ cm^{-2}, $\sigma_n \approx 10^{12}$ cm^{-2}, puddles ≈ 9 nm.

Slow method!

Differential conductance map

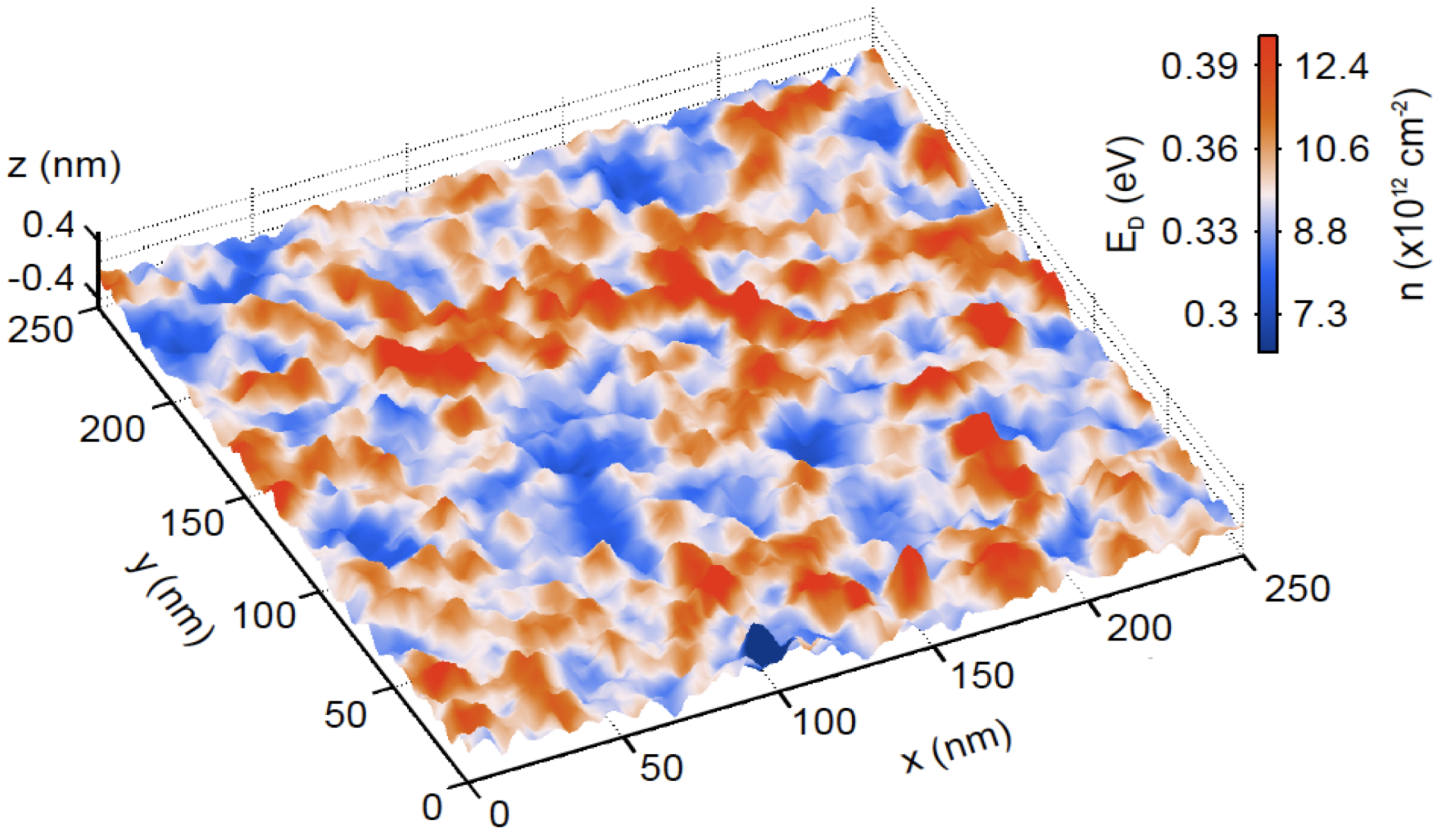

Differential conductance image translated into E_D map.

Correlations between topographic height and doping

S. Martin, S. Samaddar, A. Kimouche, J. Coraux, B. Sacépé, H. Courtois, C. Winkelmann, Physical Review B 91, 041406 (2015).

Calculating a correlation

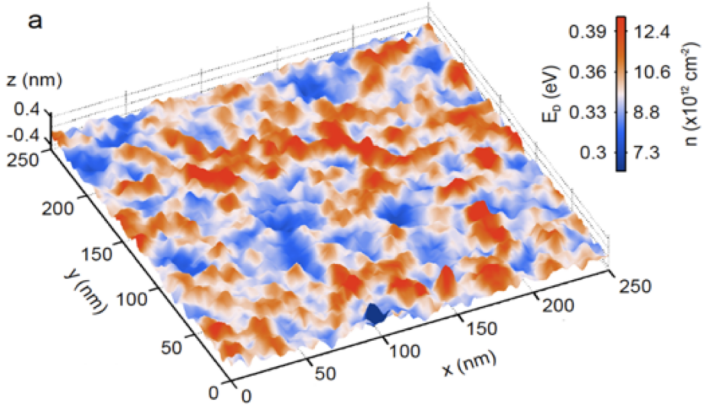

Correlation coefficient as a function of distance:

$$\chi(r) = \frac{\sum_i \left(E_D(r_i - r) - \overline{E_D}\right).\left(z(r_i) - \overline{z}\right)}{\sigma_{E_D}.\sigma_z}$$

If perfect correlation = 1, decorrelated = 0

Strong local correlations between topographic height and doping.

Interpretation: contaminants between Ir and graphene brings doping

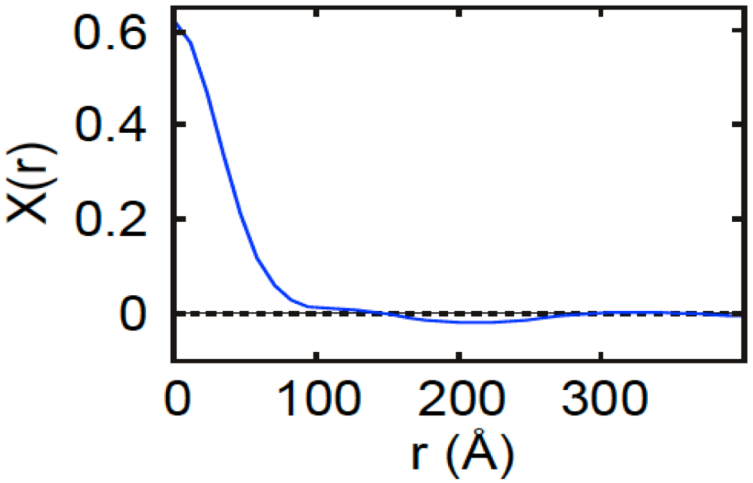

S. Martin, S. Samaddar, A. Kimouche, J. Coraux, B. Sacépé, H. Courtois, C. Winkelmann, Physical Review B 91, 041406 (2015).

Scattering interferences in graphene

Elastic scattering within graphene:

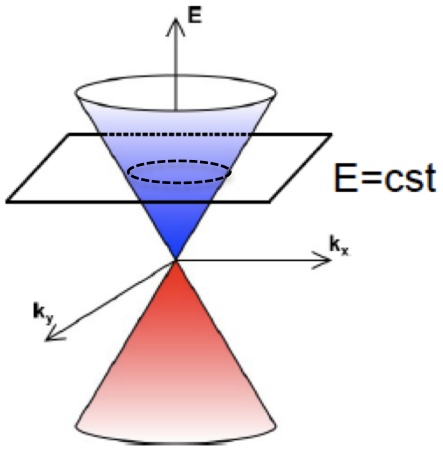

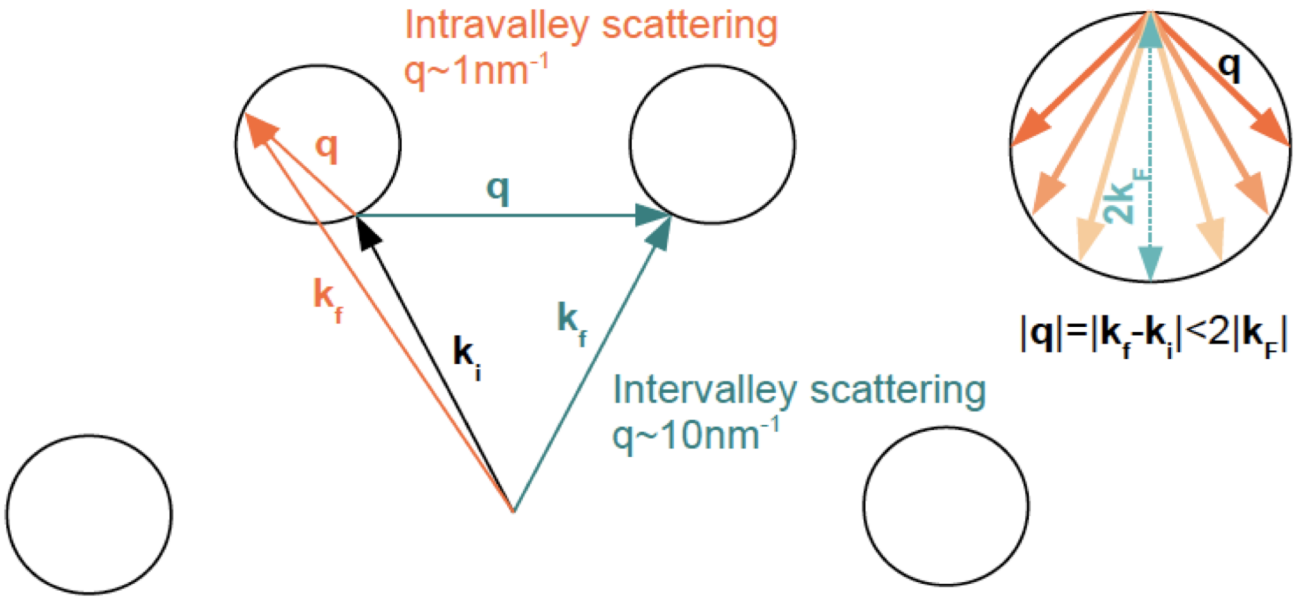

Interference between incident and scattered waves:

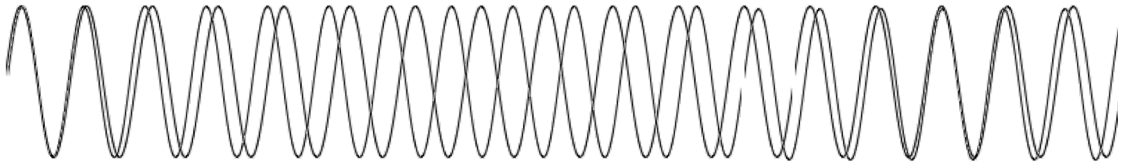

oscillations obtained at the wave-vector difference = q

Density of states inhomogeneities far from E_D

Local density of states map at varying energy.

Interferences at a scale smaller than puddles.

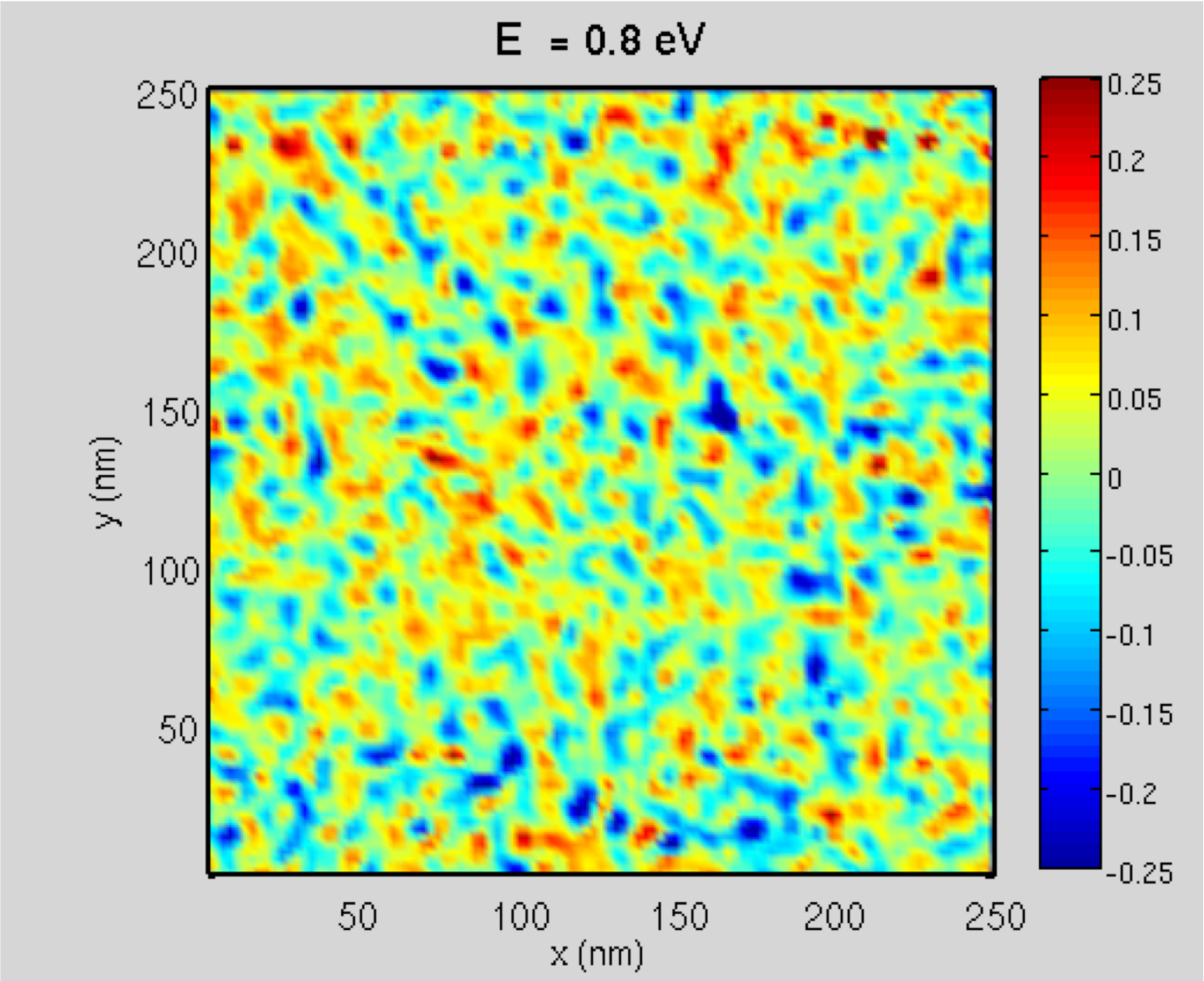

Fourier transform analysis: intravalley scattering

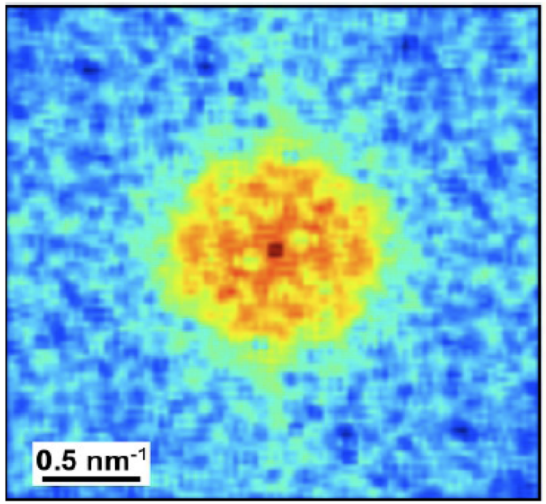

E = 15meV

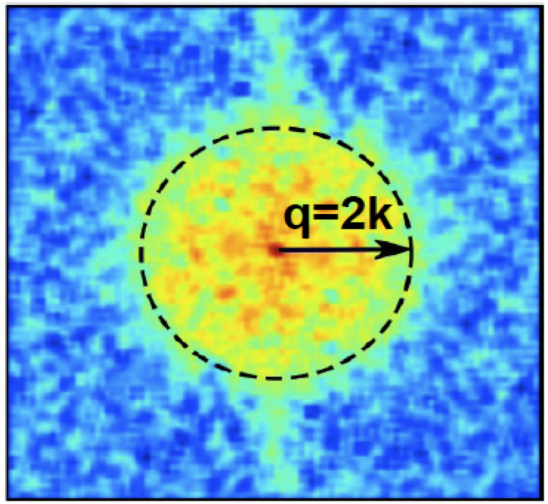

125meV

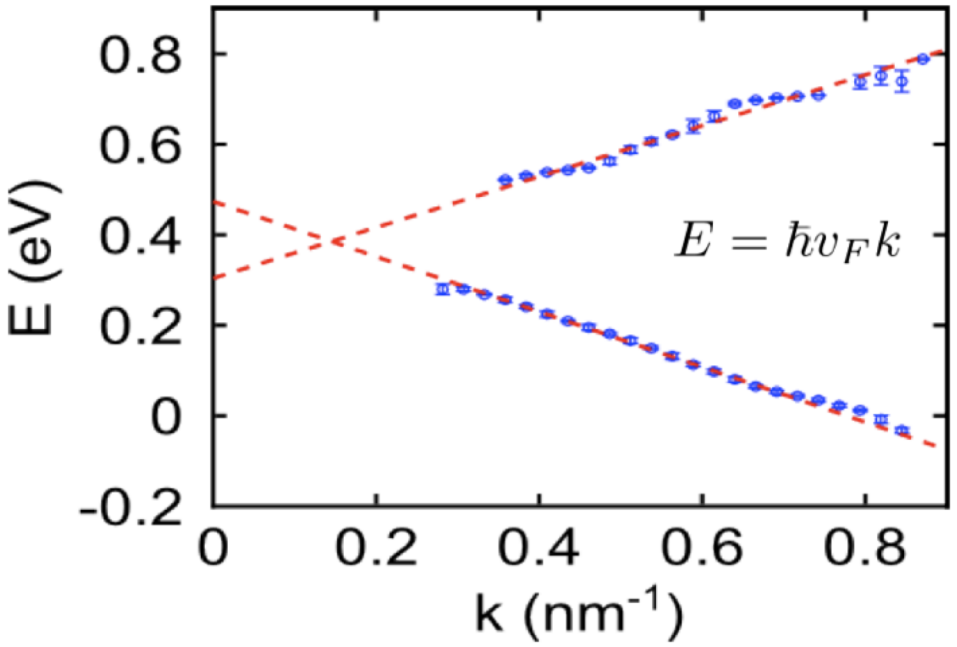

FT of qp interferences images:
disk (not a ring) with a diameter k_F

Gives access to energy dispersion relation
Linear dispersion relation: $v_F = 8.9 \pm 0.4 \times 10^5$ m/s

Chapter 4
Scanning Tunneling Spectroscopy

4.4 Single-wall carbon nanotubes

Structure

Discovered in 1991: S. Iijima et al., Nature 354, 56 (1991).

Wrapped graphene sheet with a rolling vector:

$$\vec{R} = n\vec{a}_1 + m\vec{a}_2$$

(n,m) defines the tube geometry.

n = m : armchair
m = 0 : zig-zag
n ≠ m chiral

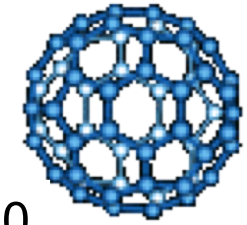

C60

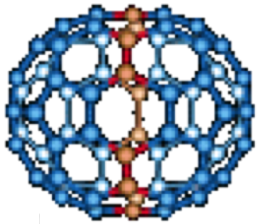

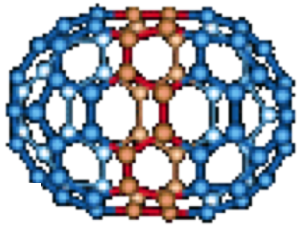

armchair

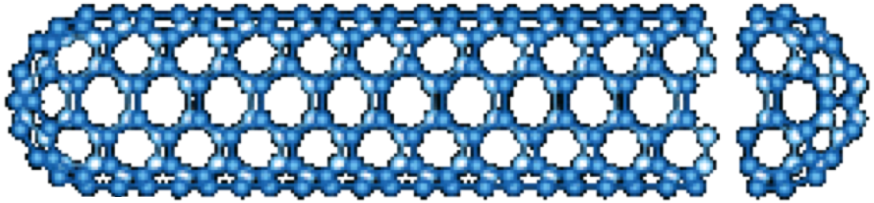

(5,5)

zig-zag

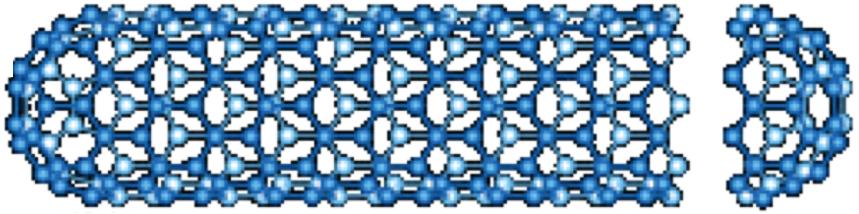

(9,0)

chiral

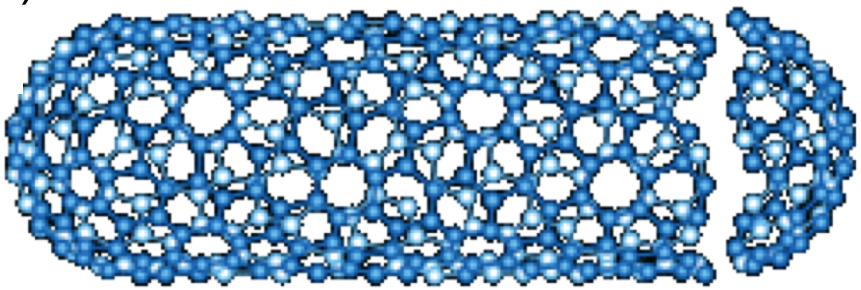

(10,5)

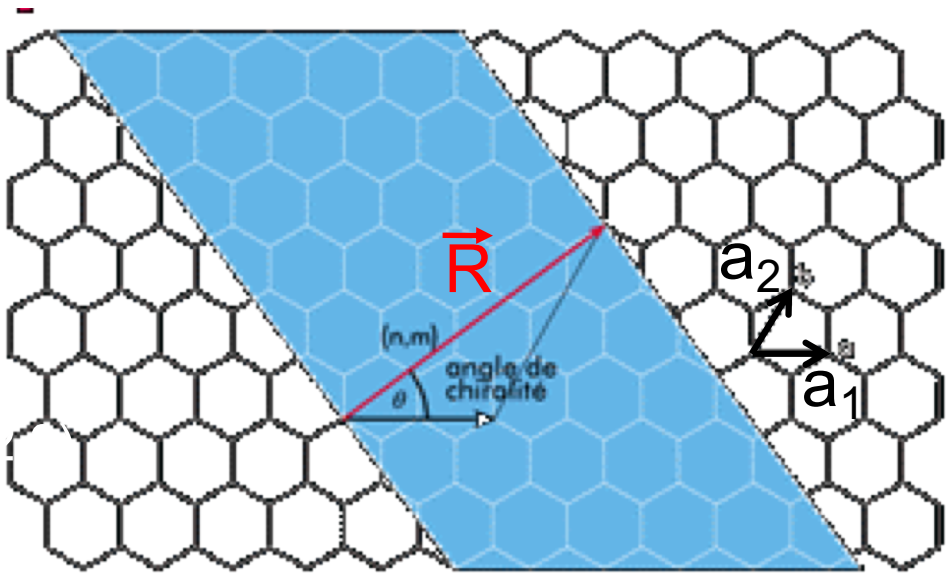

Electronic states in graphene

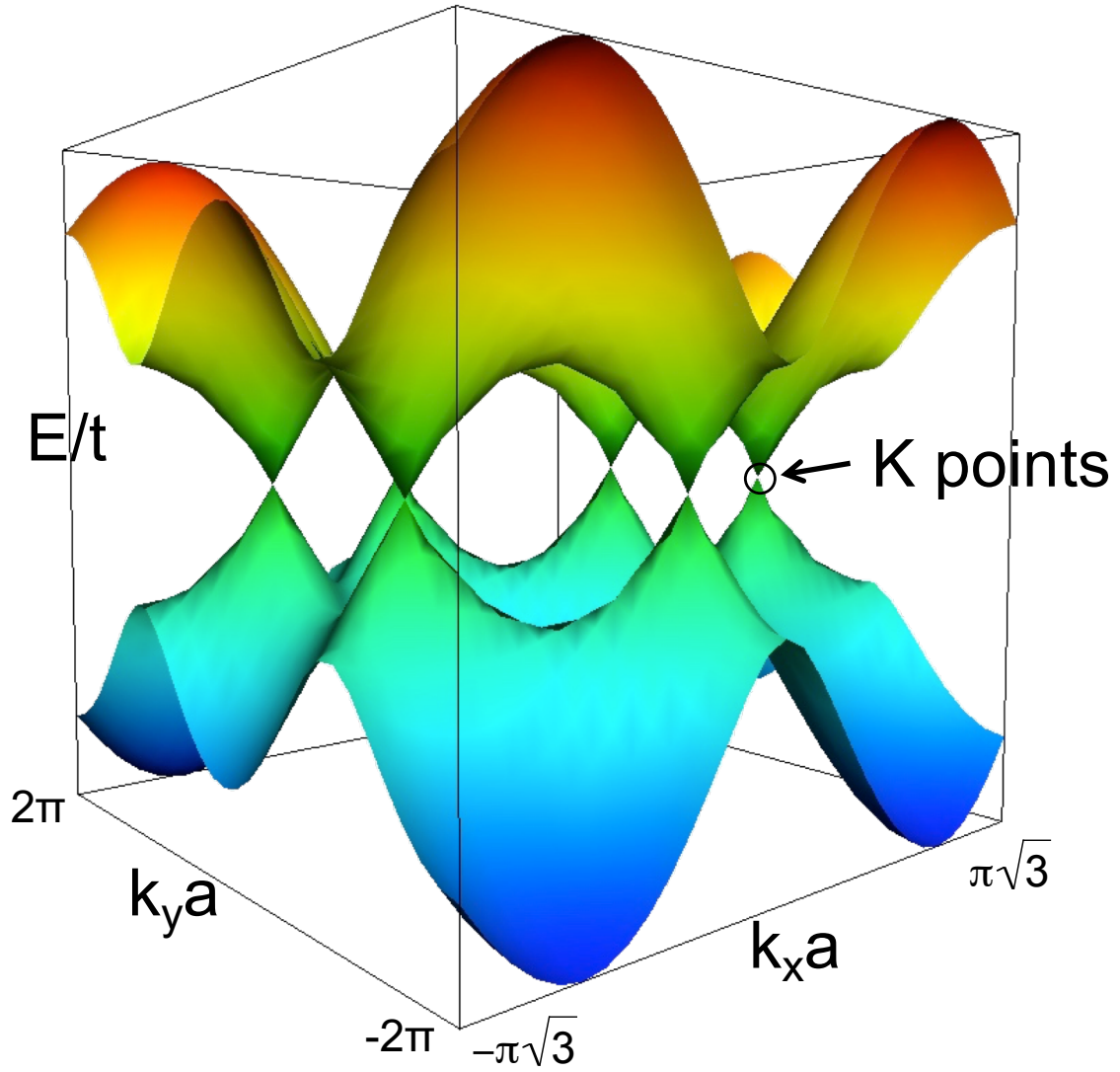

Armchair tubes are metallic

Armchair, periodic boundary condition around the perimeter:

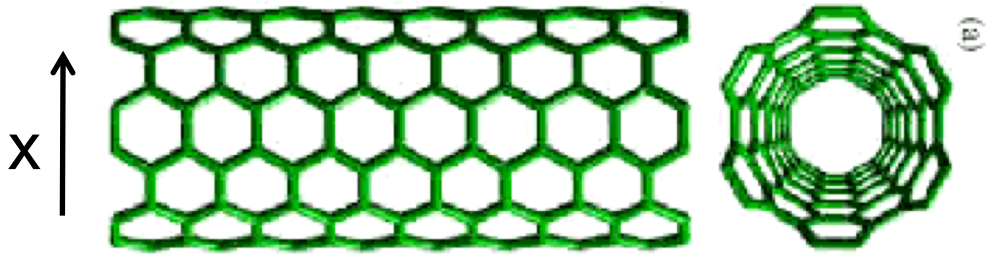

$k_x . m\sqrt{3}a = 2\pi p$ p integer

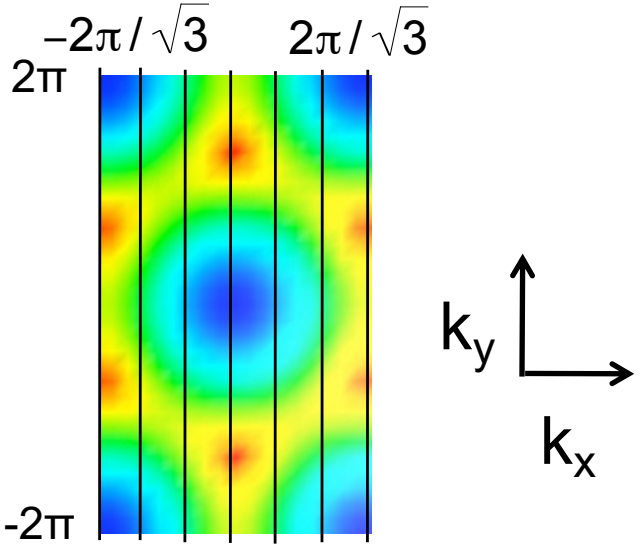

m = 3

$$k_x a = \frac{2\pi p}{m\sqrt{3}}$$

K points in red in this figure.
Selected k cross K points: metallic.

Zig-zag can be metallic or semiconducting

Zig-zag, periodic boundary condition around the perimeter:

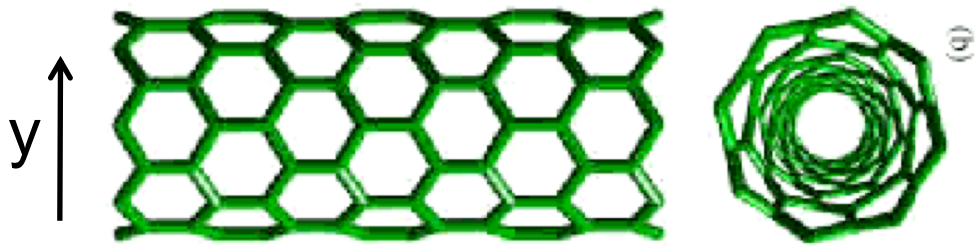

$k_y . na = 2\pi p$ p integer

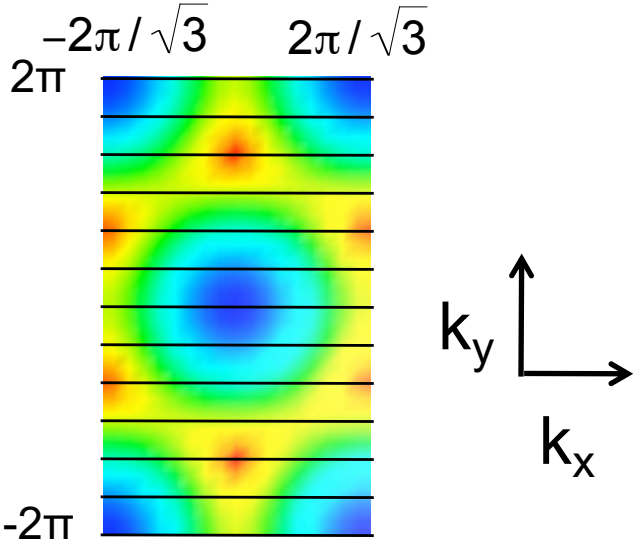

$$k_y a = \frac{2\pi p}{n}$$

K points in red in this figure.
Selected k cross K points or not, depending on n. Metallic if multiple of 3.

n = 6: metallic CNT

Zig-zag can be metallic or semiconducting

Zig-zag, periodic boundary condition around the perimeter:

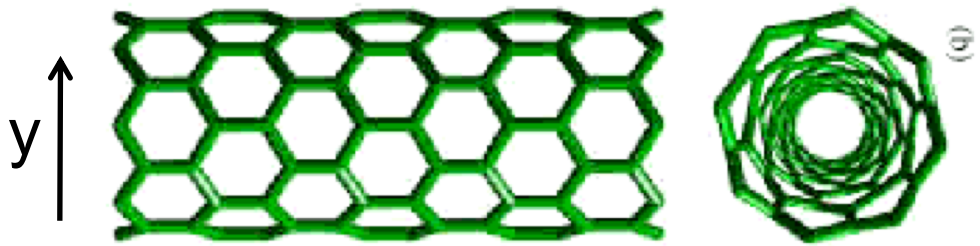

$k_y.na = 2\pi p$ p integer

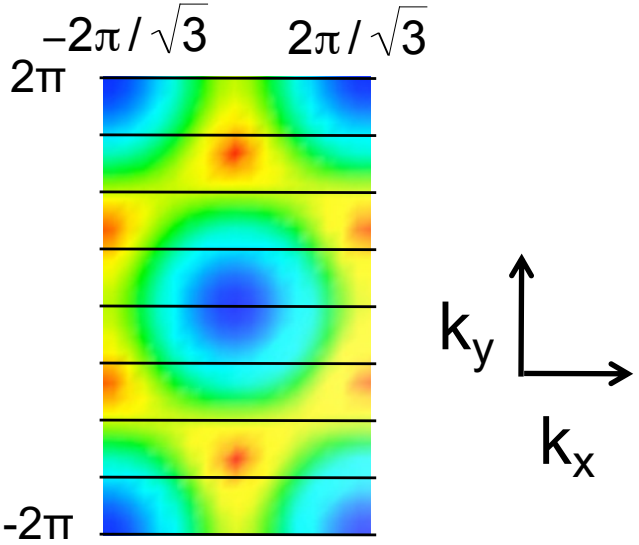

$$k_y a = \frac{2\pi p}{n}$$

K points in red in this figure.
Selected k_y cross K points or not, depending on n. Metallic if multiple of 3.

n = 4: semiconducting CNT

Chiral nanotubes …

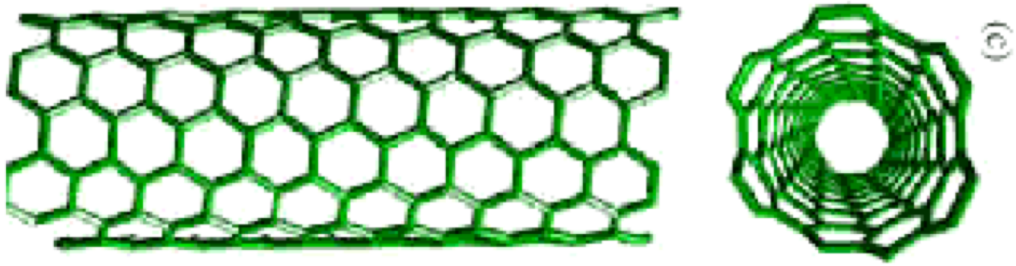

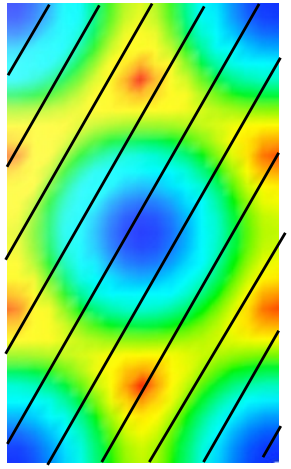

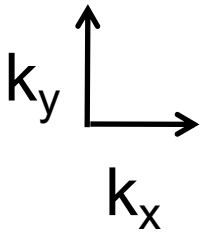

Boundary condition:

$$k_x.m\sqrt{3}a + k_y.(n-m)a = 2\pi p$$

Selected k_x,k_y lines can cross K points, depending on (m,n), in which case the CNT is metallic.

Theoretical prediction:

n - m = 3k : metallic,

n - m ≠ 3k : semiconductor.

CNT imaging

CNTs on a Au surface.

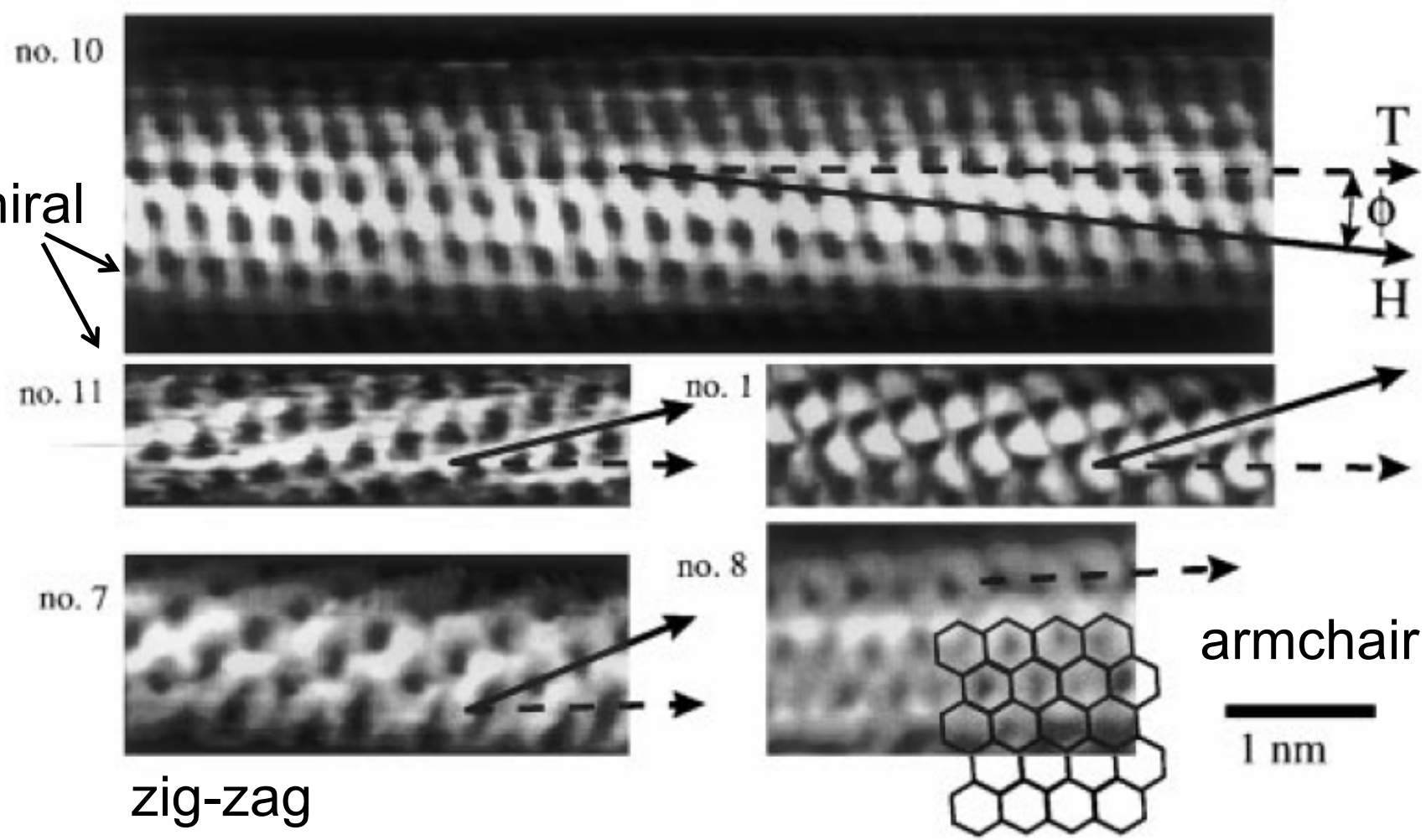

J.W.G. Wildoer, C. Dekker et al, Nature 391, 59 (1998).

CNT spectroscopy

Metallic and semiconducting tubes identified.

Armchair tubes found metallic. Statistics agrees with 1/3 of chiral ones being metallic.

Energy gap in SC tubes:

$$E_{gap} = 2\gamma a / \sqrt{3} d$$

d: tube diameter.

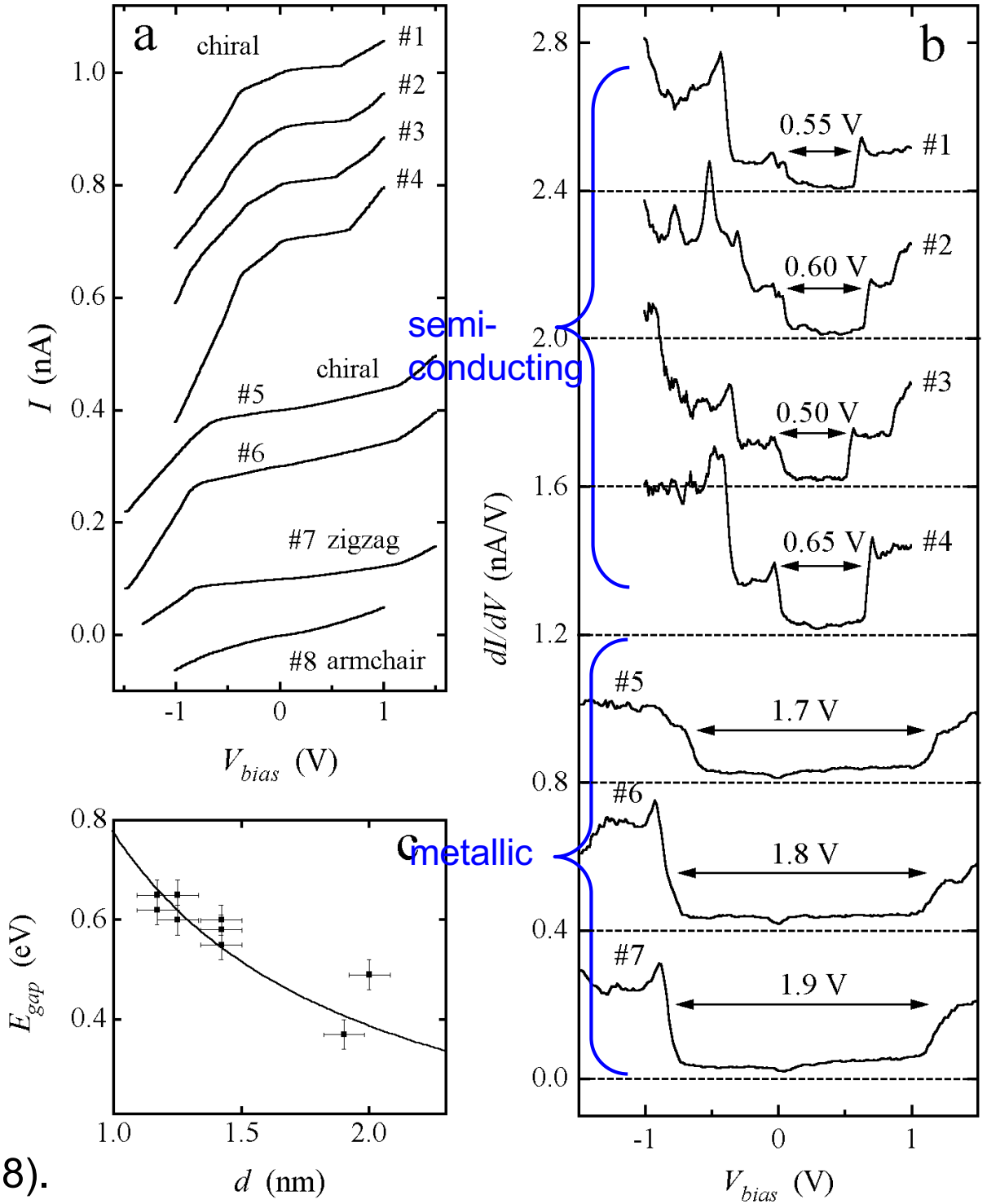

J.W.G. Wildoer et al, Nature 391, 59 (1998).

Cutting a nanotube

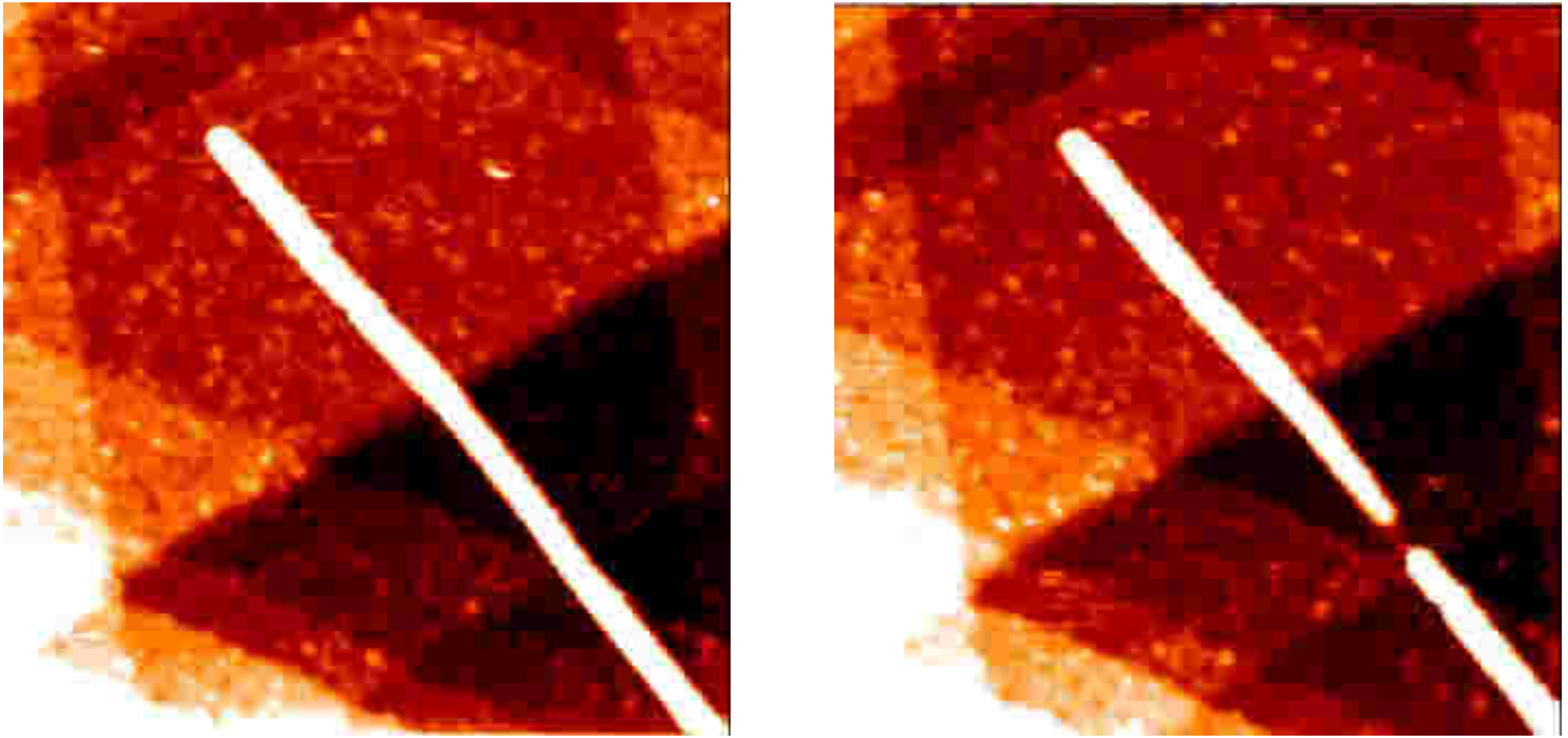

Voltage pulse (5 V) in the STM mode.

L. C. Venema, J. W. G. Wildöer, H. L. J. Temminck Tuinstra, C. Dekker, A. G. Rinzler and R. E. Smalley, Appl. Phys. Lett. 71, 2629 (1997).

Imaging electron wave functions in a CNT (1)

Armchair (metallic) tube cut with a voltage pulse:

Tunnel contact I(V) and dI/dV evolves spatially at low energy.

LDOS spatial modulation.

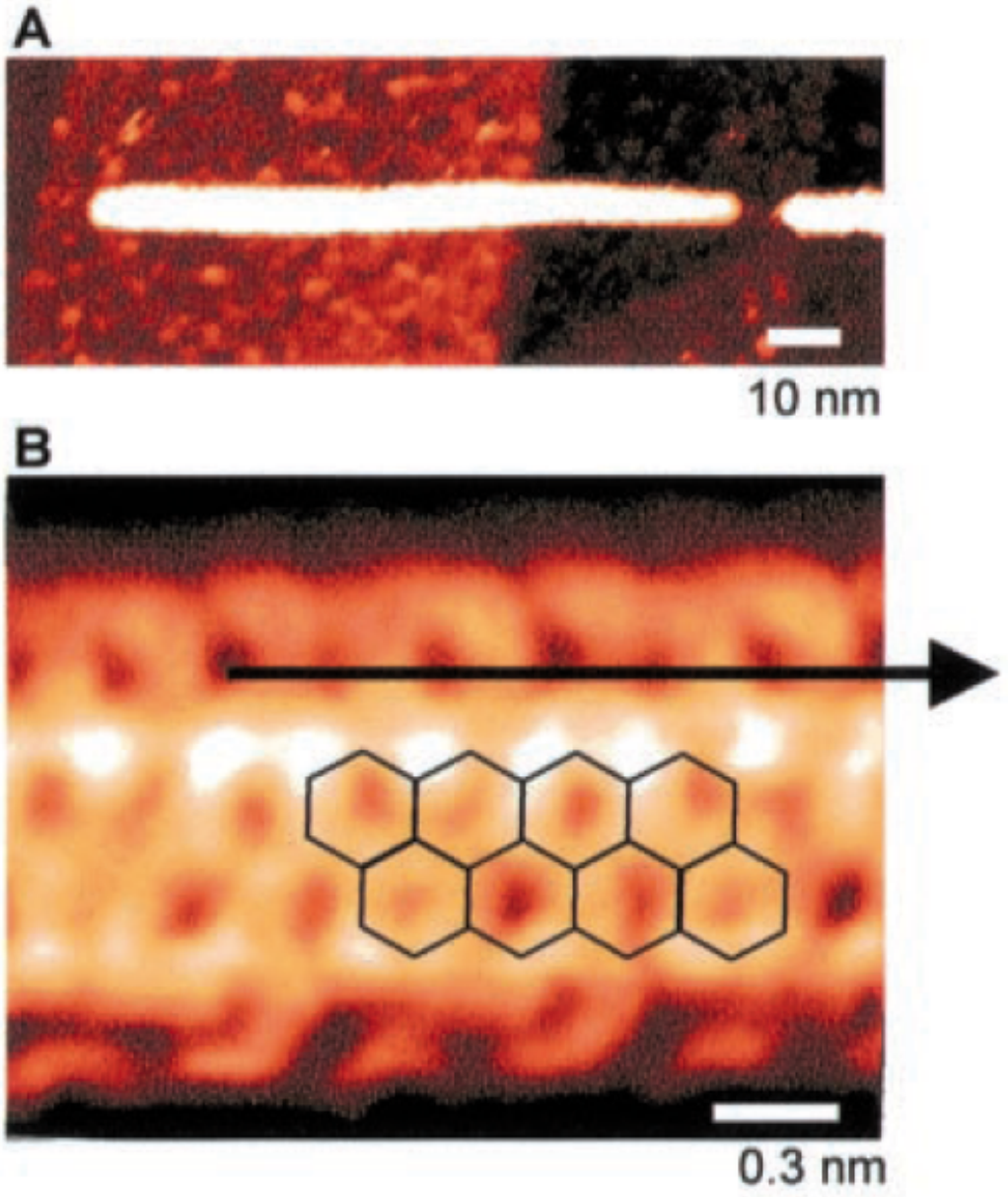

L. C. Venema et al, Science 283, 52 (1999).

Imaging electron wave functions in a CNT (2)

Period different from atomic cell size, close to Fermi wavelength: electronic standing waves.

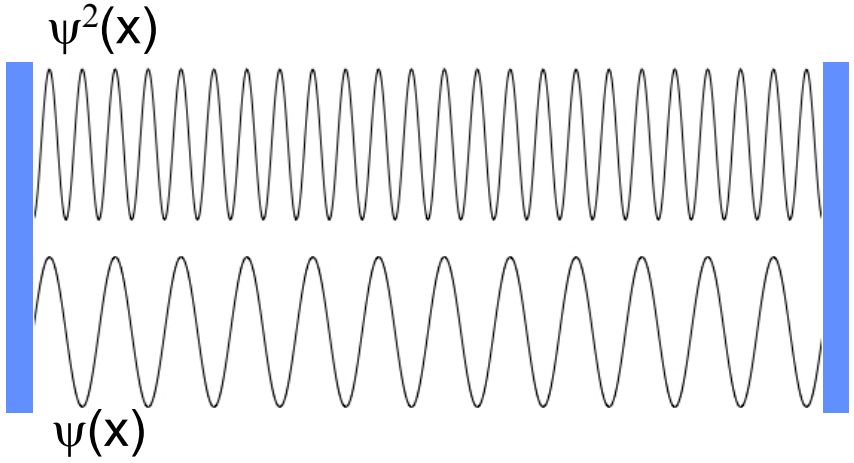

$$\psi(x) = A \sin(2\pi x/\lambda)$$

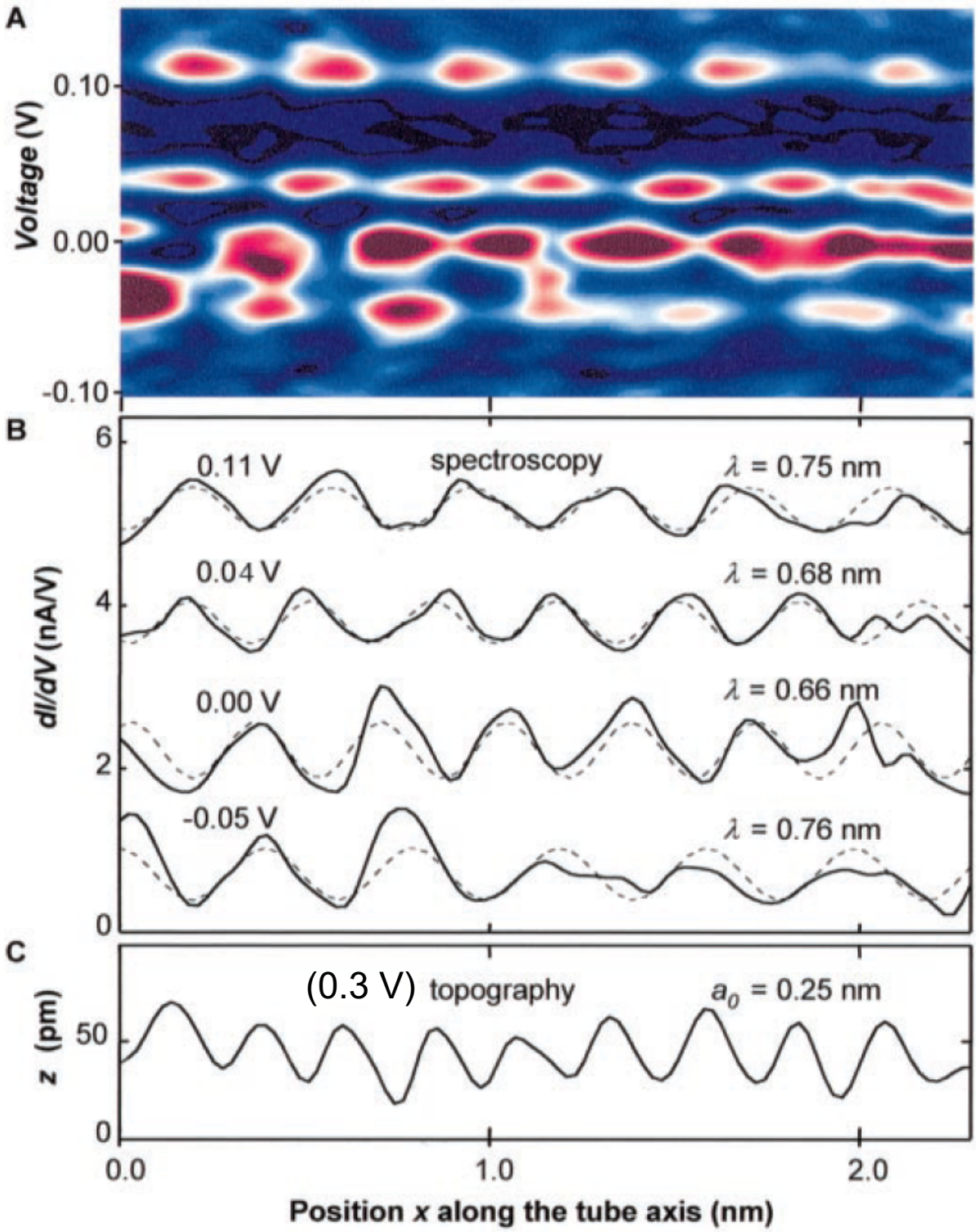

Imaging electron wave functions in a CNT (2)

Differential conductance proportional to electron density:

Fit: $\frac{dI}{dV} = G_1 \sin^2\left(2\pi x/\lambda\right) + G_0$

Textbook model of a particle in a 1D box, here about 100 e-.